

NAS-8819-FM-9614-820
CONTRACT NUMBER: NAS9-18819
LINE ITEM: 3
DRL ITEM: 3
FMI PROJECT: NAS-9614
FMI DOCUMENT: NAS-9614-4

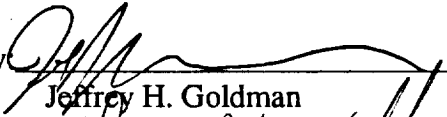
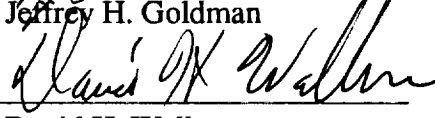
LUNAR BASE HEAT PUMP

JULY 1994

PHASE I FINAL REPORT

Prepared for:
NASA LYNDON B. JOHNSON SPACE CENTER
CREW AND THERMAL SYSTEMS DIVISION
HOUSTON, TX 77058

Prepared by:
J. Goldman
A. Harvey
T. Lovell
D. Walker
Foster-Miller, Inc.
350 Second Avenue
Waltham, MA 02154-1196
(617) 890-3200

Prepared by: 
Jeffrey H. Goldman
Approved by: 
David H. Walker

U. S. Government agencies only

SUMMARY

Several criteria were followed to select the high temperature lift (lunar base) heat pump concept. These criteria were:

1. Lowest possible overall cost including DDT&E, launch, operation, and maintenance.
2. Lowest possible overall system mass and volume, not necessarily the lowest heat pump mass and volume. This translates to the highest heat pump COP at the optimal heat rejection temperature.
3. Safest and most readily available working fluid.
4. Highest reliability through simplicity and use of proven off-the-shelf components.
5. Greatest flexibility in development.

Using these criteria resulted in three concepts, utilizing basically the same technology, for a planetary (lunar) base, a planetary (lunar) lander,

and the ground development (SIRF) unit. The three concepts are summarized in Table 1.

The planetary (base) unit is a three-stage unit utilizing R-11 (CFC-11) as the refrigerant and screw-type compressors in all three stages. Several manufacturers produce flight qualified compressors of this type, however each unit is designed and qualified for each specific application and they are considerably more expensive than off-the-shelf commercial hardware. The heat exchangers are high density, micro-fin/plate similar to those produced by the Hamilton Standard Division of United Technologies Corporation. Superheat is removed from the compressors' suction via a liquid suction heat exchanger (LSHX) ahead of the first stage and economizers and intercoolers prior to the upper stages. Heat pump control is achieved by sequencing the stages operating and the number of compressors operating within each stage. Control of the upper stages can be refined to a greater degree by using variable speed control of one or more of the compressors.

Table 1. Heat Pump Concept Summary

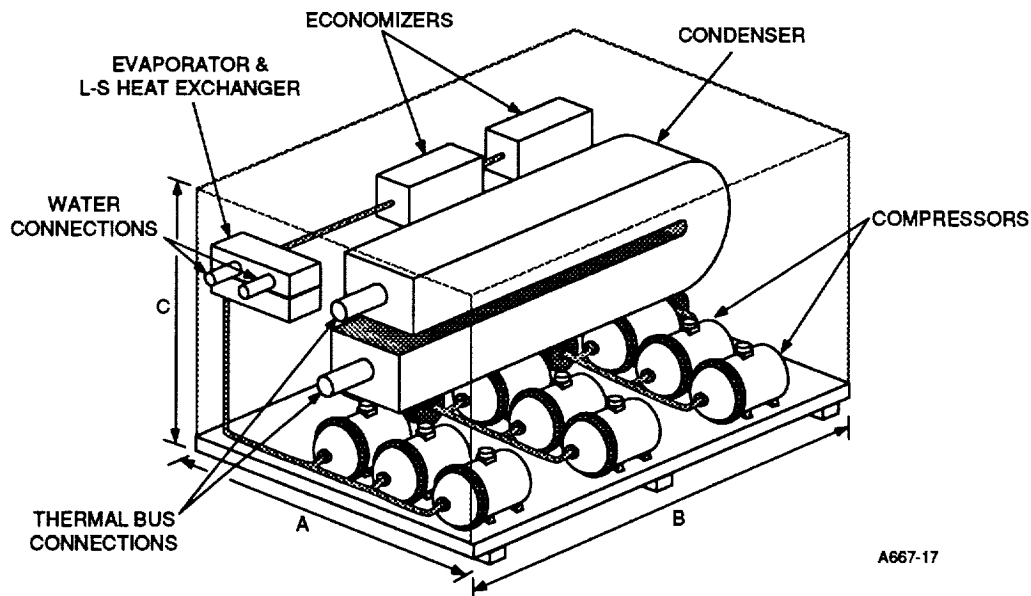
	Base	Lander	SIRF
Mass	120 kg	47 kg	NA
Dimensions	750 mm wide x 1000 mm long x 750 mm high	750 mm wide x 750 mm long x 750 mm high	1220 mm wide x 1520 mm long x 910 mm high
Volume	563,000 cc	420,000 cc	1,688,000 cc
Fluid	R-11 → R-123	R-11 → R-123	R-11 → R-123
Cycle	Three-Stage	Two-Stage	Two-Stage
Compressors	Screw	Screw and Rotary	Scroll and Rotary
Predominant Heat Exchanger Type	Flight-Qualified Plate-Fin	Flight-Qualified Plate-Fin	Commercial Plate-Fin
Control Scheme	Multiplexed compressors with variable speed	Same	Same

The lander heat pump is a down-sized version of the base unit. The refrigerant, heat exchangers, and control scheme are similar and based on the same technology. The first-stage compressors are similar screw-type to the base unit, however the second-stage are replaced by positive displacement, rotary-type (rolling piston) compressors because small enough screw compressors are not available. This option is not possible with the base unit due to its larger capacity and reliability requirements.

Figures 1 and 2 show the package layout and schematic of both the base and lander heat pumps.

To deliver 25 kW of cooling with a minimum of system mass, the condenser should operate at 382K and the radiator should operate at 378K. With our concept the $COP_{Cooling}$ will be approximately 56 percent of the Carnot ideal, the heat pump mass will be approximately 120 kg, the power system and radiator system mass will be approximately 868 kg, and the total system will be approximately 988 kg, excluding interconnecting plumbing.

The ground development (SIRF) unit uses similar technology to the base and lander. However it is packaged on an open pallet to allow frequent component changes, and uses commercial off-the-shelf components. This allows less expensive development and evolution toward the flight system. The SIRF is a two-stage system like the lander, but the first-stage compressors are commercially available scroll compressors that closely emulate the discharge pressure characteristics of screw compressors. This lowers the cost with a minimum of affect on the evolution to flight-type screw compressors. Three Hitachi L500BL scroll compressors will meet these requirements. The second stage, similarly to the lunar lander, will use rotary compressors, however only two are needed. Two Mitsubishi RL5538EP compressors will meet these requirements. The heat exchangers are commercial plate-fin (ITT Standard) type, again to lower the development costs. The control scheme is similar to the base and lander units, however the controller will be an industrial process controller, again to reduce development cost. Figures 3 and 4 show the SIRF package layout and schematic.



A667-17

	A mm (in.)	B mm (in.)	C mm (in.)	WEIGHT (kg)
Lander	750 (30)	750 (30)	750 (30)	45
Base	750 (30)	1000 (40)	750 (30)	120

Figure 1. Lunar Heat Pump Package Layout

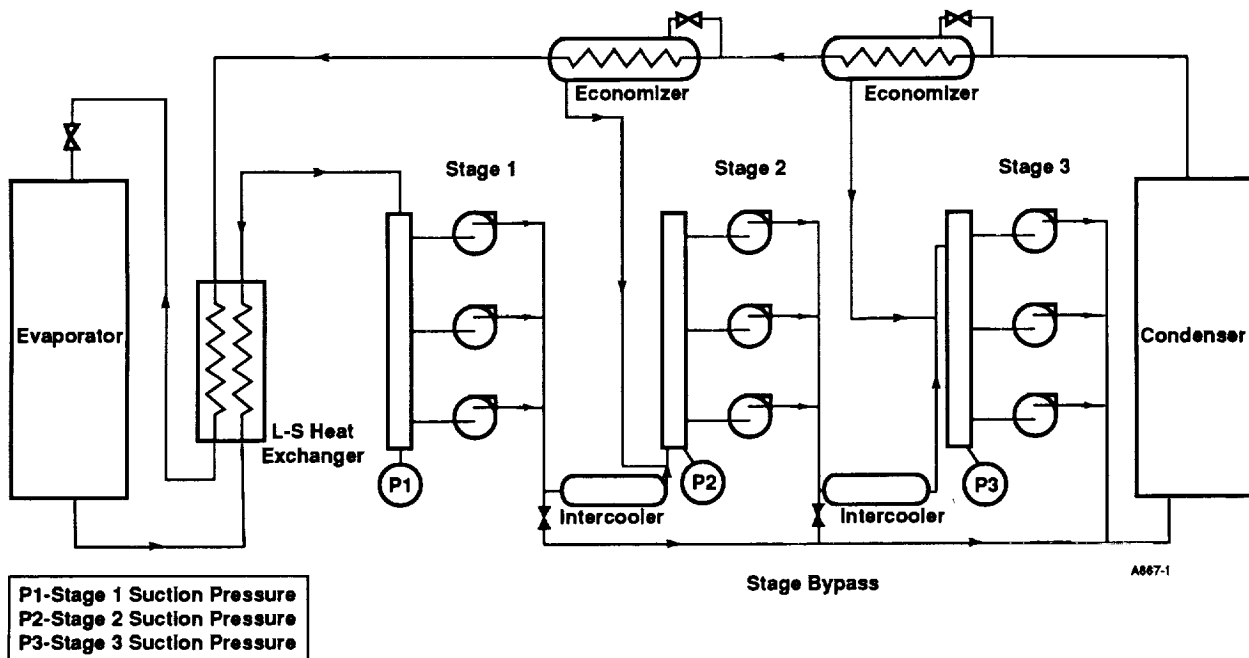


Figure 2. Flow Diagram of the Lunar Heat Pump

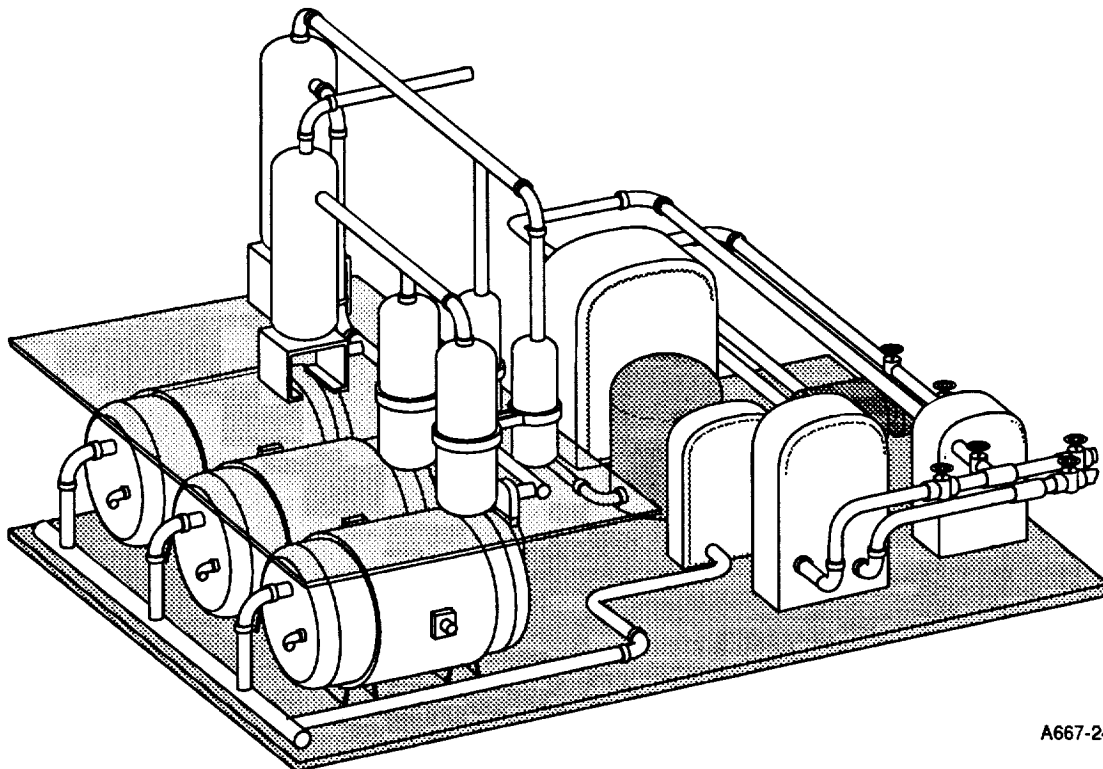


Figure 3. Layout of SIRF Heat Pump

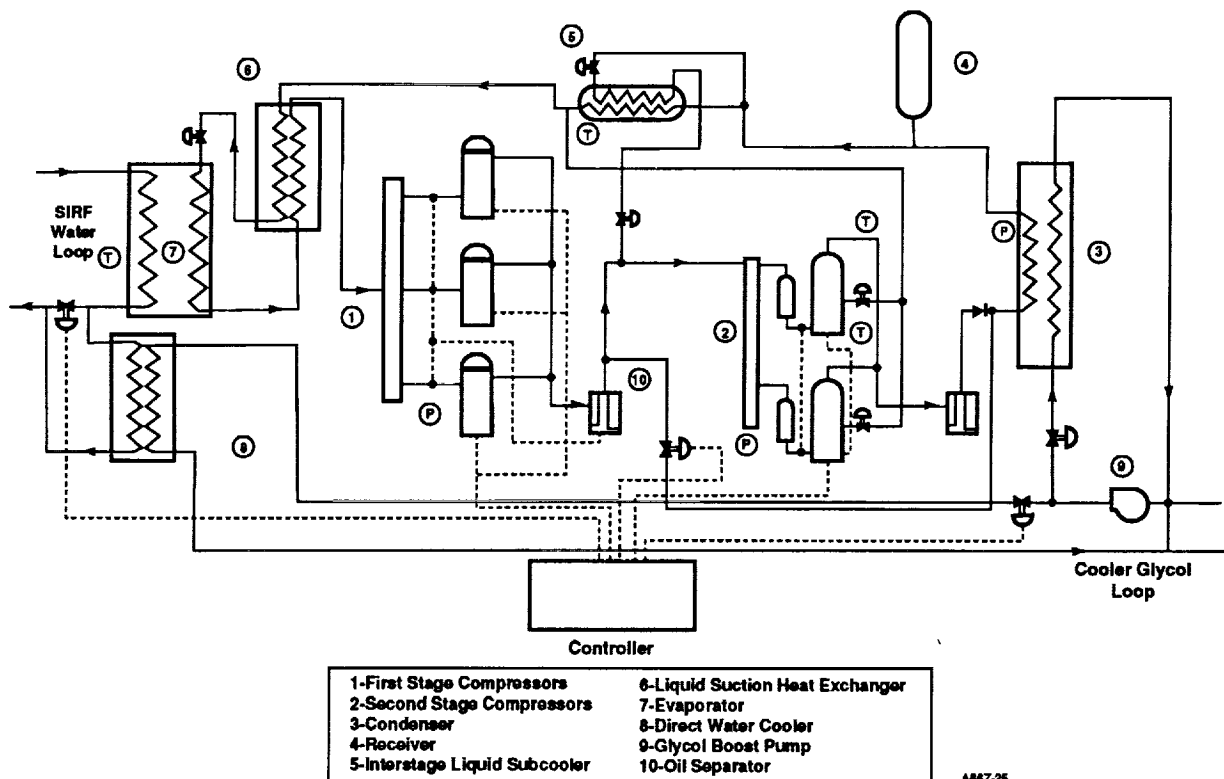


Figure 4. SIRF Heat Pump Diagram

Using similar technologies between the flight heat pumps and the SIRF ground test unit was a

high priority, however there are significant differences due to cost. These are summarized in Table 2.

Table 2. Common Technologies and Differences

	Lunar	SIRF
Thermal rejection loop	2-phase	Glycol-water
Maximum rejection temperature	Base 378K Lander 387K	360K
Working fluid	R-11	R-11 (can operate with HCFC-12 or future HFC)
Cycle	Base - three-stage Lander - two-stage	Two-stage
Hardware	Flight-qualified	Off-the-shelf
Compressors	Base - Screw lander - Screw and rotary	Scroll and rotary
Heat exchangers	Plate - Fin with micro channels high surface/volume	Plate - Fin Commercial grade
Control scheme	Multiplexed compressors combined with variable speed (load variation) Staging (condenser temperature change)	Same as Lunar

1. INTRODUCTION

A heat pump is a device which elevates the temperature of a heat flow by means of an energy input. By doing this, the heat pump can cause heat to transfer faster from a warm region to a cool region, or it can cause heat to flow from a cool region to a warmer region. The second case is the one which finds vast commercial applications such as air conditioning, heating and refrigeration. Aerospace applications of heat pumps include both cases.

In the first case, when heat can be rejected directly to space by radiation, a heat pump can reduce the amount of radiator area required by elevating the rejection temperature. If the heat pump can be operated efficiently enough that the radiator weight savings is more than the extra weight of the heat pump and its power system, then there is a net benefit. Since radiator weight savings go up and heat pump performance goes down with increasing temperature lift, there is a tradeoff in deciding how high to raise the heat rejection temperature.

Some aerospace applications fall into the second case where heat is rejected (often by radiation) to a surrounding thermal environment which is warmer than the area to be cooled. One example of this is a lunar base habitat near the moon's equator. Although NASA has sent humans to the moon before, they were never sent for extended periods of time. The Apollo missions were relatively short in duration and were conducted during the early part of the lunar day/night cycle. Hence the Apollo lunar module Thermal Control Systems (TCS) could reject waste heat via evaporative cooling through a water boiler. During future missions to the moon, or to other planets, the crew and support equipment will be exposed to more severe thermal environments for longer periods of time. Therefore, using a consumable fluid such as

water for thermal control will no longer be feasible. A heat pump of some type must be used to enable rejection of moderate temperature waste heat to these more severe environments. For example, a lunar base TCS will collect waste heat from the crew habitat at a temperature of about 275K. That waste heat must then be elevated to a temperature above that of the effective thermal sink temperature (i.e., local environment) in order to enable its rejection. For a lunar base near the equator, this will require a heat pump with a relatively high temperature lift.

The NASA Johnson Space Center is currently developing a Systems Integration Research Facility (SIRF) to provide system-level integration, operational test experience, and performance data that will enable NASA to develop flight-certified hardware for future planetary missions. A high lift heat pump is a significant part of the TCS hardware development associated with the SIRF.

The high lift heat pump program discussed here is being performed in three phases. In Phase I, the objective is to develop heat pump concepts for a lunar base, a lunar lander and for a ground development unit for the SIRF. In Phase II, the design of the SIRF ground test unit is being performed, including identification and evaluation of safety and reliability issues. In Phase III, the SIRF unit is manufactured, tested and delivered to NASA.

The following actions were taken to meet the Phase I objectives and to provide adequate data to select the optimum heat pump concept.

1. Conduct a systems optimization study to determine the rejection temperature that minimizes the overall power generation

and heat rejection system mass, not necessarily the heat pump's mass.

2. Conduct a tradeoff study of refrigerants and thermodynamic cycles to determine which combination yields the highest $COP_{Cooling}$ at the optimal heat rejection temperature.
3. Research and select the major components, compressor and heat exchangers, that can be used to implement the thermodynamic cycle selected. Special attention is paid to using the same technologies for the SIRF and flight heat pumps.

4. Generate a package concept for the components selected, including mass and volume estimates.

5. Identify the technology similarities and differences between the SIRF and flight units in order to identify the steps necessary to evolve to flight configuration.

Performing the above steps led us to the conclusions and recommendations included herein. The following sections describe each step.

2. SYSTEM OPTIMIZATION

The first step of this program was to determine the radiator rejection temperature that optimizes the system mass. To do this, optimization curves of system mass versus radiator rejection temperature were generated. Several assumptions were made in this analysis:

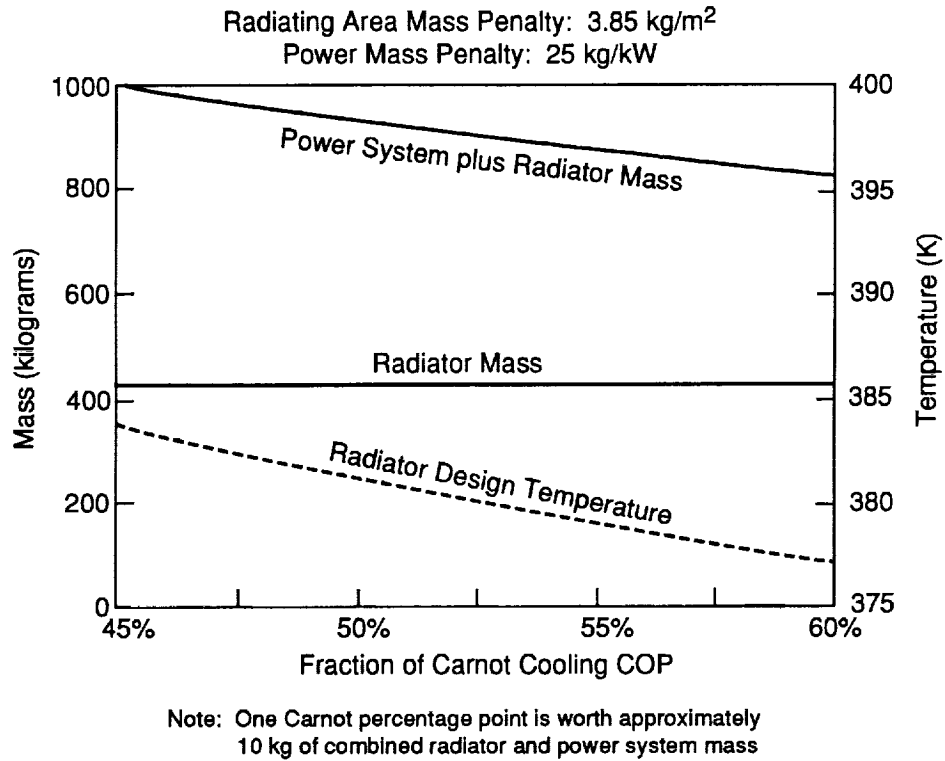
1. The application was a lunar base habitat near the equator with a maximum environment temperature of 325K and a minimum environment temperature of 80K at night.
2. The system is modular and each module of the system will reject 5 kW (thermal) from the living quarters.
3. Radiator Area Mass Penalty (RAMP) = 3.85 kg per square meter of RADIATING surface as specified by NASA.
4. Power Mass Penalty (PMP) = 25 kg per kilowatt (electrical) for daytime power at a lunar base presuming a solar photovoltaic power source as specified by NASA.
5. The tradeoff study used power system mass and radiator system mass only. All other component and system masses were assumed to be zero and not entered into the tradeoff study.
6. The heat pump performs at a constant fraction of the Carnot ideal as the condensing temperature changes.
7. The radiator must be large enough to provide all night cooling without the heat pump operating due to extremely high nighttime power mass penalties.

This analysis shows that the design point is controlled by the area required for passive heat

rejection during the lunar night. Then, given this nighttime fixed radiator size, the noontime optimum design point depends only upon the coefficient of performance ($COP_{Cooling}$) of the heat pump. A more efficient heat pump requires less power and allows the fixed radiator to operate at a lower temperature. The lower radiator operating design temperature results from less compressor power needing to be rejected as heat. The lower system mass results from the reduced need for power.

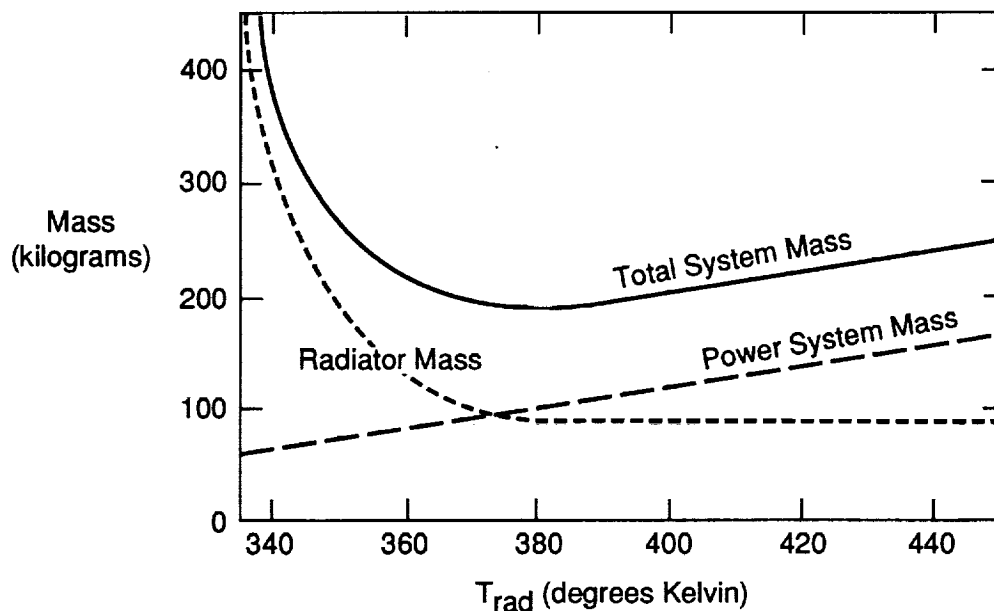
For COPs in the range of 45 to 60 percent of the Carnot cooling efficiency (1), the optimum noontime radiator design temperature varies from 381K down to 374K. Simultaneously, the total system mass (power supply plus radiators) varies from 1000 kg down to 810 kg. Figure 5 shows the relationship between System Mass and Fraction of Carnot Cooling COP.

The supporting calculations to this analysis are included in Appendix A. In these, we initially calculated the necessary radiator area for passive operation during the lunar night. Next, for a variety of heat pump COPs, the noontime radiator temperature was varied between 335K to 450K, total system weight was calculated, and the system with the lowest total mass was selected as optimum. In most cases, if the system was designed without regard for passive night operation, a smaller radiator and higher operating temperature would seemingly yield slightly lower total system mass. To operate such a system at night would require power storage, forcing a much larger total system weight (except in the case of a nuclear power supply). Figures 6 and 7 illustrate how optimum radiator operating temperatures were chosen to yield minimum system mass with heat pump efficiencies of 50 and 70 percent of Carnot. Together they show that total system mass is a function of both COP and radiator rejection temperature.



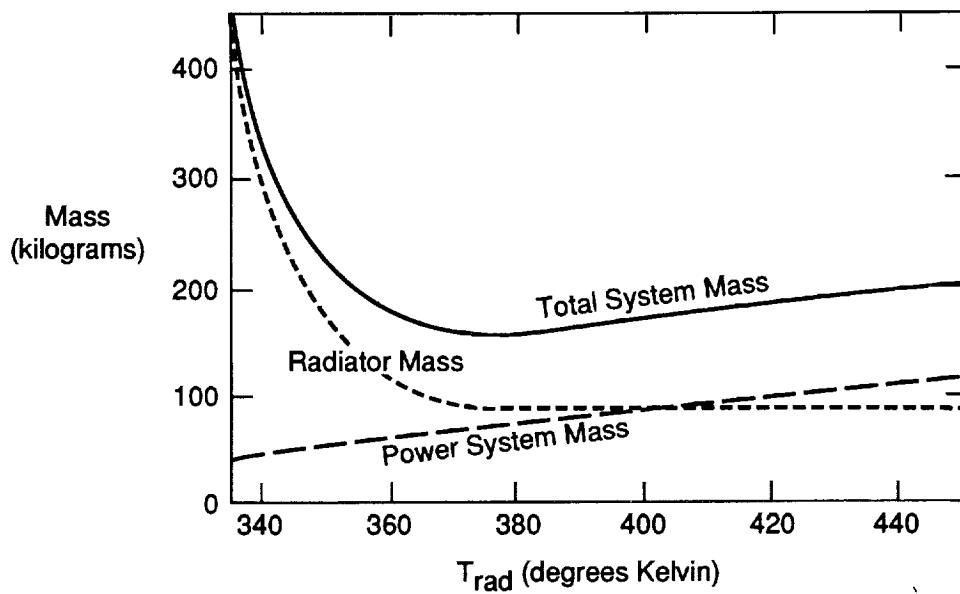
235-M94 013-5

Figure 5. System Mass versus Fraction of Carnot Cooling COP



235-M94 013-6

Figure 6. Mass versus Radiator Temperature: 50 Percent of Carnot Cooling COP



235-M94 013-7

Figure 7. Mass versus Radiator Temperature: 70 Percent of Carnot Cooling COP

This analysis shows the temperature and efficiency ranges within which a successful lunar base heat pump should operate. Accordingly,

refrigerants and refrigeration cycles able to meet these rather stringent requirements were examined.

3. REFRIGERANT AND THERMODYNAMIC CYCLE SELECTION

Analyses of many refrigerant fluids in refrigeration cycles were performed in order to determine the most efficient heat pump cycle and refrigerant. In general, the analyses show that several different fluids, in realistic heat pump cycles, could perform at about 50 percent of the Carnot cooling COP. A few fluid/cycle combinations may approach 56 percent. Calculations also showed that, for systems-level analysis, one may accurately assume a constant percentage (e.g., 51 percent) of the Carnot cooling COP across the range of radiator temperatures of interest.

Many refrigerants were considered and specifically analyzed in over a dozen specifically-optimized vapor-compression cooling cycles. Leading thermodynamic

contenders for the lunar base heat pump are listed in Tables 3 and 4. The order of preference is the same for the lunar base heat pump and the ground based prototype. However, the actual prototype performance estimates would be different because of the slightly lower temperature lift and the less than optimal component specifications dictated by off-the-shelf commercial hardware.

The Coefficient of Performance (COP) was calculated for all cycle and refrigerant combinations as the dimensionless ratio of *cooling* performed to *power* required. Unlike many heat pump applications, the lunar base requires the net cooling delivered by a heat pump, not its net heat rejection. The temperatures used to determine the Carnot COP_{Cooling} were the internal evaporator and the

Table 3. Single Refrigerant Cycles

Refrigerant	Configuration	% Carnot COP
CFC-11	Three-stage, base	56
	Two-stage, SIRF	55
Ammonia	Three-stage, base	50
HCFC-123	Two-stage, base	50
	Two-stage, SIRF	40

Table 4. Cascaded Cycles

Upper Stage Refrigerant	Configuration	Lower Stage Refrigerant	COP	% Carnot
Water	Two-stage	HCF-123a	1.27	51
Water	Two-stage	Ammonia	1.25	50
HCFC-123a	Two-stage	Ammonia	1.20	48

internal condenser temperatures. This is somewhat different from the classical definition, but it does isolate the heat pump and therefore eliminates the efficiency factor of the Thermal Control System heat exchangers.

3.1 Performance as a Constant Fraction of Carnot

A real heat pump was assumed to perform at some fixed percentage of the Carnot cooling COP during the general analysis of system weight versus radiator temperature. The analysis was then repeated for COPs varying from 20 to 70 percent of Carnot. One leading realistic candidate cycle (R-123a in a two-stage arrangement) was checked against this simple assumption. Specifically, across a range of possible design temperatures, the effect of condenser temperature on COP was checked. Table 5 shows the outcome of this detailed cycle analysis.

Over the range of condenser temperatures of interest, the estimated COP stays a nearly constant percentage of the ideal Carnot cooling COP. Thus, the approximation used to analyze overall system mass proves a very good estimate. This estimate therefore continued in use for overall system analysis. Estimated heat pump performance proved about 50 percent of the ideal Carnot COP_{Cooling}.

3.2 Fluid and Cycle Selection

The search for the "perfect" lunar refrigerant included old and new, and common and obscure

fluids. Some simple thermodynamic concepts helped organize both the search for and the evaluation of the refrigerants. The simplest and first criterion to apply in the fluid search was critical temperature. Any fluid with a critical temperature below the optimum lunar condenser temperature (about 383K) fails as a refrigerant for this vapor-compression heat pump application.

The next thermodynamic criterion applied was actual COP in a well-chosen, realistic cycle. Sensitivity of COP to small changes in the cycle state points was then checked. Refrigerants with high COPs that are also insensitive to small changes warranted further study.

Refrigeration cycles to suit each refrigerant were then designed. Simple guidelines dictated what elements should make up an optimum refrigeration cycle for any given fluid. To understand how to optimize refrigeration cycles, tailor-made for each fluid, requires some background. A qualitative description of the process is described. This explanation will help interpret the numerical results which will be presented last.

3.3 The Ideal Carnot Refrigeration Cycle

Given ideal equipment, a perfect Carnot refrigeration cycle could operate within the vapor-liquid dome of a typical refrigerant. Figure 8 illustrates this concept on a temperature-entropy diagram. Notice that virtually all points within the cycle occur within the "dome," the

Table 5. Constant Fraction of Carnot COP_{Cooling} with Temperature Lift

Condenser Temperature	Radiator Temperature	Estimated C.O.P.	Carnot C.O.P.	% Carnot
375K	371K	1.44	2.75	52.3
378K	374K	1.39	2.68	51.9
381K	377K	1.34	2.61	51.3
383K	379K	1.30	2.54	51.2
385K	381K	1.28	2.50	51.2

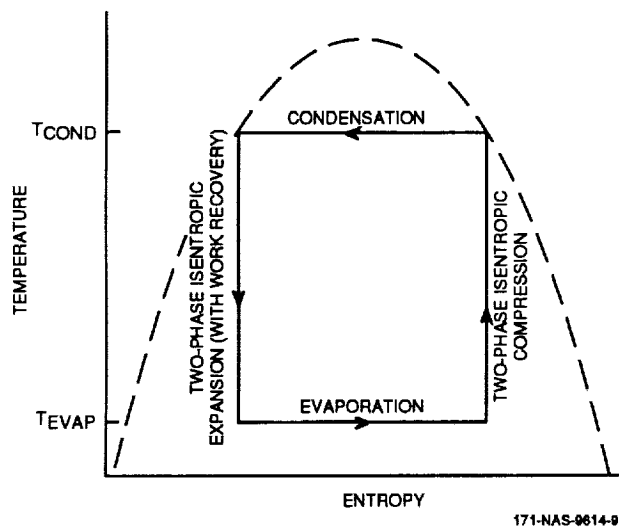


Figure 8. Ideal Carnot Refrigeration Cycle

two-phase region of the state diagram. All heat rejection occurs at a constant high temperature; all heat acceptance occurs at a constant low temperature. A perfect compressor pressurizes, with no losses, a vapor-liquid mixture. A perfect turbine starts with saturated liquid and expands it, with no losses, as a vapor-liquid mixture, extracting useful work.

The simple academic diagram of Figure 8 was used as the standard against which to judge any real cycle. The comparison showed where real cycles incurred their worst losses and thus suggested realistic improvements.

3.4 Realistic Refrigeration Cycles

Figure 9 schematically shows the equipment which forms the basis of all practical vapor-compression refrigeration cycles. An evaporator accepts heat, vaporizing low pressure liquid refrigerant, to give the desired cooling effect. A compressor takes vapor from the evaporator and delivers high-pressure gas to the condenser. The condenser rejects heat, cooling and ultimately liquefying this gas. The hot liquid condensate cools as it flashes through an expansion valve to the evaporator. The flashed, two-phase mixture enters the evaporator to repeat the cycle.

Used with this basic refrigeration system, real fluid performance departs from the Carnot ideal.

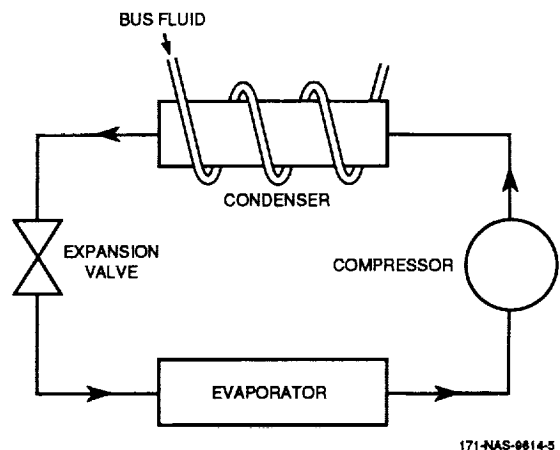


Figure 9. Schematic of Single-Stage Refrigeration System Components

The specific departure from Carnot varies with fluid properties. The method used to optimize a cycle for a fluid depends on where in the cycle the fluid departs from ideal. Real fluids fall into two general property categories, wet compression and dry compression. Each category degrades the ideal Carnot cycle in its own way and requires its own cycle optimization. The next section discusses those categories.

3.5 Wet and Dry Compression Refrigerant Categories

Refrigerants break roughly into two groups: wet compression and dry compression.

Dry Compression Refrigerants

Dry compression refrigerants exhibit single-phase (or superheated) isentropic compression starting from any saturated vapor condition. The dome shape of such refrigerants on a temperature-entropy state diagram qualitatively mirrors that shown in Figure 10. As explained below, such refrigerants inherently have large superheat at the compressor discharge. Examples of this type of refrigerant are ammonia, water, and HCFC-22.

Wet Compression Refrigerants

Wet compression refrigerants exhibit two-phase isentropic compression starting from most saturated vapor conditions. Figure 11 shows the

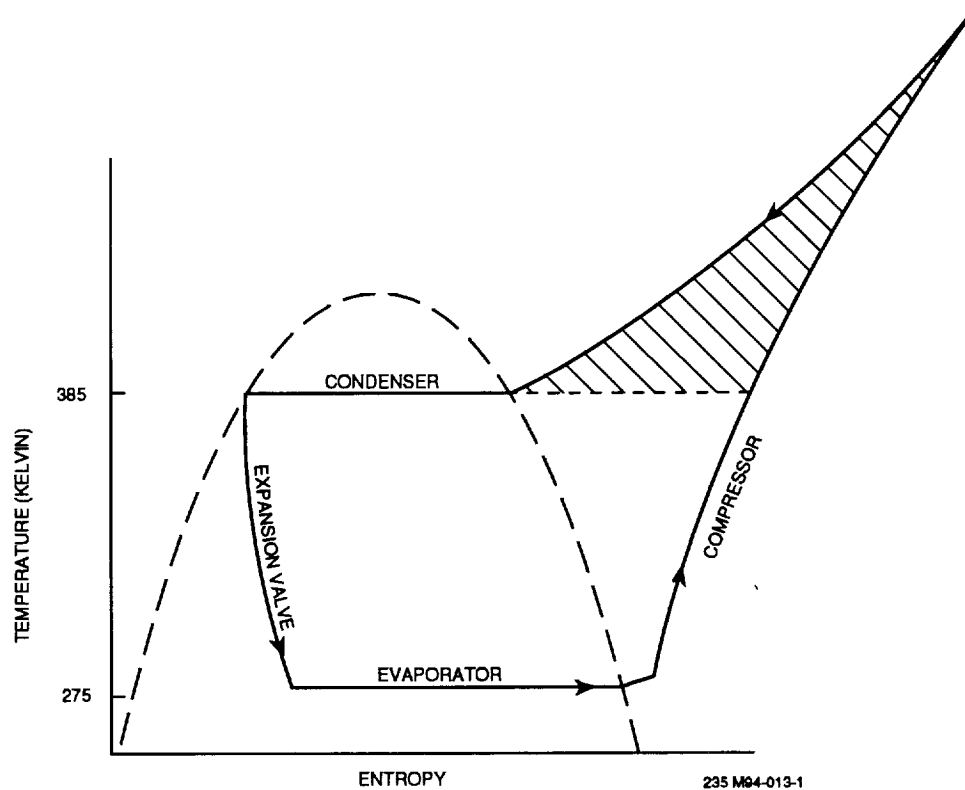


Figure 10. Typical Single-Stage Refrigeration Cycle for Dry Compression Fluids

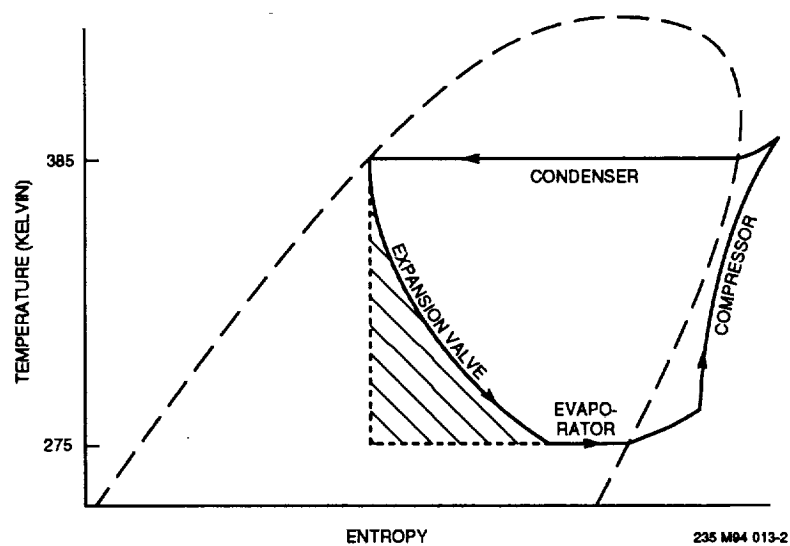


Figure 11. Typical Single-Stage Refrigeration Cycle for Wet Compression Fluids

dome shape of a typical wet compression fluid on a temperature-entropy diagram. Note that, unlike the dome of the dry compression refrigerant, the wet compression dome tilts to the right. As explained below, such refrigerants inherently have large throttling losses (high vapor production during a flashing process). Examples of this type of refrigerant are HCFC-123 and HCFC-134a.

All refrigerants fall into one of these two categories, although some classify as borderline, exhibiting neither strongly wet nor dry compression (2,3). This classification method was also found useful for clarifying the fluid/cycle selection process in this program. Note that "wet" or "dry" compression both refer only to the fluid categories as defined above, not to the actual compression process in specific proposed cycles. A "wet compression" refrigerant, with sufficient suction superheat, will remain in a dry state through the whole compression process. Allowing any wet compression to occur will usually degrade compressor and hence, cycle performance. Accordingly, refrigerant cycles that were designed with "wet compression" fluids were designed with sufficient suction superheat that the refrigerant stayed dry during the compression process.

The two basic refrigerant types behave differently in a typical vapor-compression refrigeration cycle. Dry compression refrigerants inherently exhibit small throttling losses, but large compressor superheat. Wet compression refrigerants show the opposite behavior. Namely, they have large throttling loss (i.e., a large entropy gain and loss of cooling effect), but little compressor superheat. These different behaviors require different refrigeration cycles to attain optimum performance.

3.6 Dry Compression Fluid Departures from the Carnot Ideal

Dry compression fluids degrade the Carnot ideal with high compressor superheat. Figure 10 shows a typical, realistic, single-stage refrigeration cycle using a dry compression refrigerant. Note the several departures from the ideal Carnot cycle. The high compressor discharge temperature creates the largest departure from Carnot. This superheat means

heat rejection over a large range of temperatures and therefore causes cycle inefficiency. The shading on Figure 10 marks the extra work created by this major excursion from an ideal Carnot cycle. Cycle optimization must address this disadvantage inherent in most dry compression fluids.

On the other hand, the throttling losses for dry compression fluids create only a minor excursion from the Carnot ideal, as also illustrated in Figure 10. Finally, aside from compressor head-cooling (when available) the thermodynamicist must accept non-isentropic compression as a fact of life.

3.7 Wet Compression Fluid Departures from the Carnot Ideal

Wet compression refrigerants degrade the Carnot ideal with large throttling losses. Figure 11 illustrates a typical, realistic, single-stage refrigeration cycle using a wet compression refrigerant. Again, note the various excursions from the Carnot ideal. The large throttling loss creates the single most major departure from the Carnot ideal. The large throttling inefficiency means loss of cooling effect per unit mass of refrigerant circulated through the evaporator. Thus, the compressor must circulate more mass flow, and use more power, for any desired cooling rate. The shading on Figure 11 marks the lost cooling effect of the throttling process. Alternatively, this area represents unrecovered work from vapor expansion in the flashing process. Cycle optimization for wet compression fluids must specifically address this inherent disadvantage.

Other features of wet compression fluids give only minor excursions from the Carnot ideal. Note how little superheat occurs at the compressor discharge. The cycle rejects very little heat above the condenser temperature. Figure 11 also shows that if no evaporator superheat occurred, the compression would go two-phase. Practical compressors lose efficiency quickly when a liquid-vapor mixture occurs internally. Insufficient superheat at the compressor suction can thus ruin the thermodynamic cycle performance of wet compression fluids.

3.8 Wet Compression Fluid Cycle Optimization

The simultaneous need for evaporator superheat and for increased cooling effect suggests a very simple cycle enhancement for wet compression fluids. Namely, cold vapor leaving the evaporator can subcool hot condensate prior to the expansion valve. Figure 12 schematically shows a "liquid suction

heat exchanger" added to the basic vapor-compression cycle for that purpose.

3.8.1 Liquid Suction Heat Exchanger (LSHX)

Figure 13 shows the effect of liquid suction heat exchange on a refrigerant cycle using a wet compression fluid type. Note the added cooling effect in the evaporator. Much less mass flow

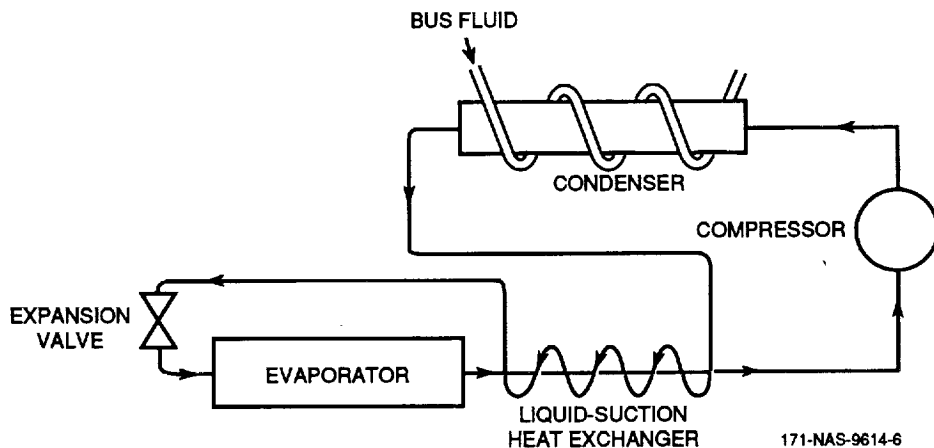


Figure 12. Schematic of Single-Stage Refrigeration System with Liquid Suction Heat Exchanger

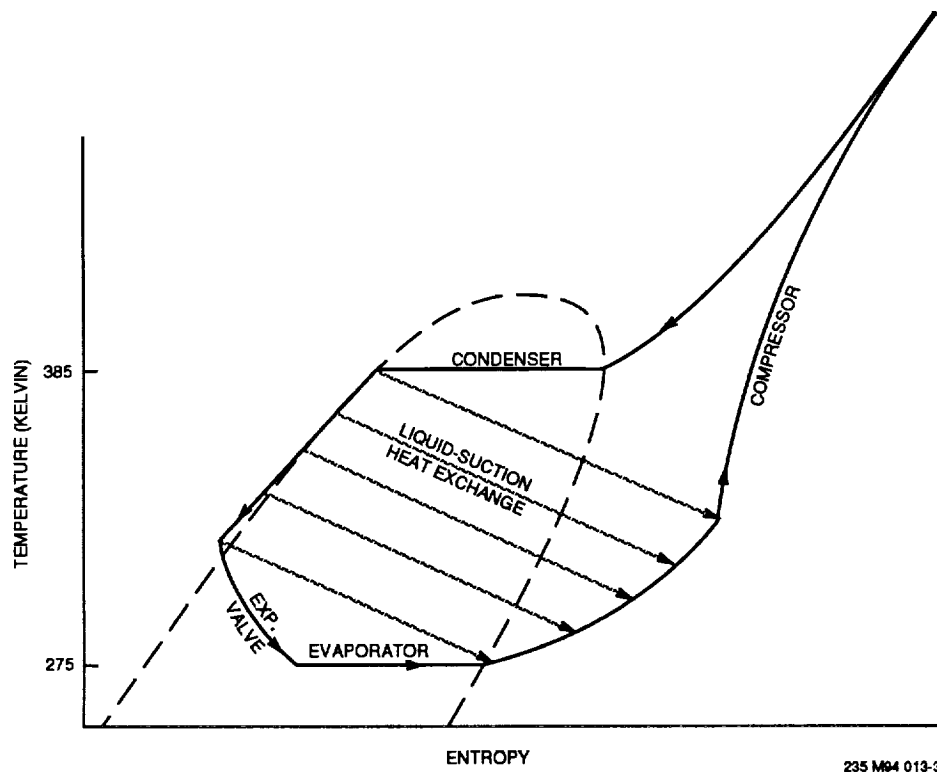


Figure 13. Single-Stage Refrigeration Cycle with Liquid Suction Heat Exchanger for Wet Compression Fluids

need circulate to provide any given level of cooling. Note also the high compressor discharge temperature. Such large superheats do not necessarily occur with all wet compression refrigerants when the cycle includes a liquid suction heat exchanger. Nevertheless, many useful wet compression refrigerant cycles show large superheats with a liquid suction heat exchanger installed because:

1. The fluid may not class as a strong wet compression refrigerant, so it superheats quite readily.
2. For wet compression fluids, condensate subcooling helps more than the resulting superheat hurts.

An optimum thermodynamic cycle for most wet compression fluids will, therefore, include as much liquid suction heat exchange as possible, regardless of compressor superheat. Compressor lubrication concerns, however, do demand some restraint from cycle designers.

The lunar base heat pump application involves a substantial temperature lift, from 275K to about 383K. This large lift means any realistic single stage compressor inefficiency will show up as considerable superheat, even with a wet compression fluid.

This analysis shows that many refrigerants perform poorly with the large temperature lift and the high condenser temperature required of the lunar base heat pump. The qualitative reasons explaining why some wet compression fluids fail and how to improve the mediocre performers will be discussed first with detailed, quantitative results discussed later. Fluids with critical temperatures above, but close to, the design condensation temperature give very poor cooling performance. Qualitatively, these fluids' vapor-liquid domes are just too narrow at such high temperatures. As refrigerants, they have little cooling effect when throttled to the low evaporator pressure. Similarly, many refrigerants (particularly the new CFC replacements) simply have narrow domes. Figure 11, for example, shows a wet compression refrigerant type. Now visualize a narrower dome and then mentally add (to the already tilted dome) a high temperature lift to a high

condensing temperature. A throttling process from the saturated liquid point will reach the evaporator temperature with almost no cooling effect remaining. In fact, some wet compression refrigerants have, over this range, throttling losses so bad that the "evaporator" would receive superheated, low pressure vapor, immediately ready for the compressor. Such a cycle would consume power and offer no cooling.

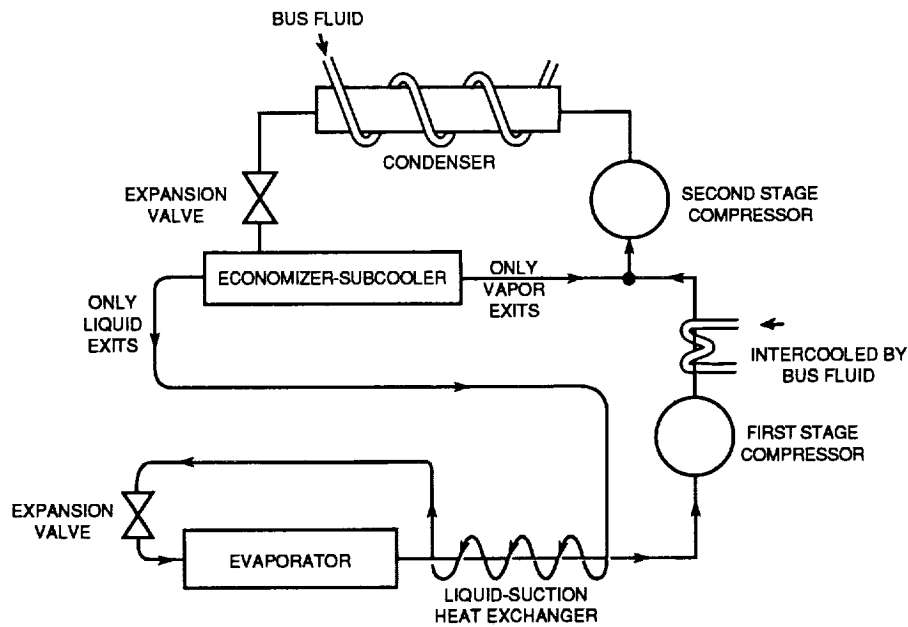
Not all wet compression fluids performed poorly in this analysis. A few showed promise in realistic single-stage cycles with liquid suction heat exchange. These almost always exhibited compressor discharge temperatures above 475K. Special oils can handle such temperatures. Standard industry refrigeration practice, however, avoids temperatures above 420K. When hotter than this, common oils lose their lubricity and the compressors soon break down.

3.8.2 Two-Stage Cycles

Multistage cycles are typically used to lower high compressor discharge temperatures and to simultaneously improve the refrigeration performance. Therefore, the best performing single-stage refrigerants were analyzed in a two-stage cycle. Figure 14 shows a schematic diagram of a two-stage wet compression fluid refrigeration system. In addition to the second-stage compressor, two new pieces of equipment appear in this diagram, the economizer-subcooler and the intercooler, both at the first-stage compressor discharge. These items are discussed in more detail in following sections. Figure 15 shows the Temperature-Entropy diagram for this cycle.

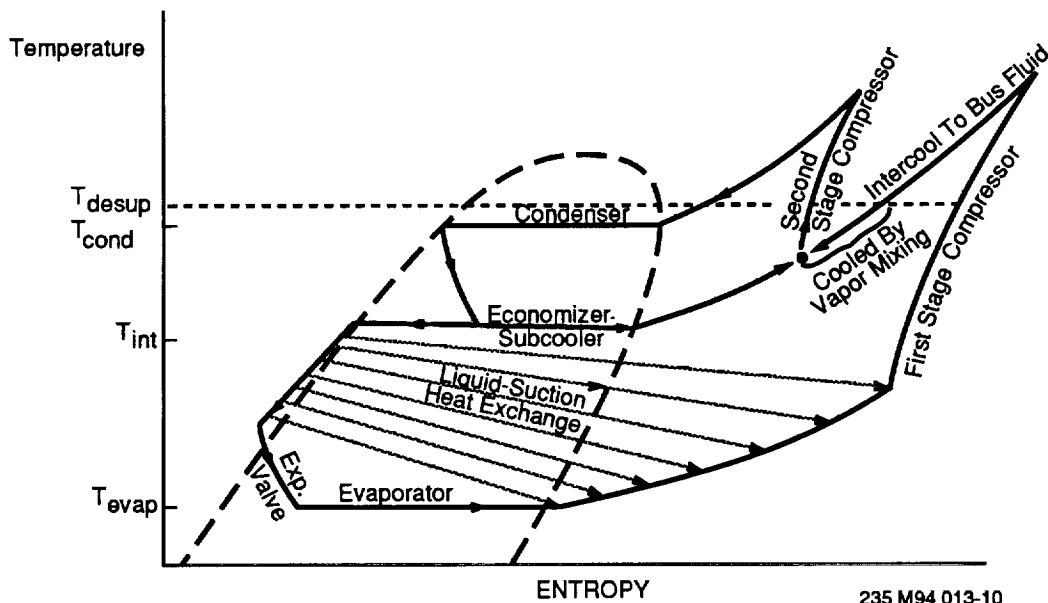
Figure 15 shows lowered compressor discharge temperatures, compared to the single-stage cycle of Figure 13. Note the increased cooling effect in the evaporator. Both the second-stage compressor power and its discharge temperature are reduced by first intercooling the first stage discharge and then by mixing it with the economizer vapor, removing more superheat.

A typical intermediate temperature is 350K. In reality, the optimum interstage saturation temperature and associated pressure vary with refrigerant and liquid suction heat exchanger



171-NAS-9614-10

Figure 14. Schematic of Two-Stage Refrigeration System with Economizer-Subcooler and Liquid Suction Heat Exchanger



235 M94 013-10

Figure 15. Two-Stage Refrigeration System with Economizer-Subcooler and Liquid Suction Heat Exchanger

effectiveness. However, the COP does not change significantly with interstage saturation temperature. Nevertheless, interstage saturation temperatures were chosen to optimize COP for each refrigerant studied.

3.9 Advanced Refrigeration Cycle Equipment

Liquid suction heat exchangers, economizer-subcoolers and intercoolers were referred to in

previous sections. Intercoolers and the economizer-subcoolers apply to multistage cycles of either wet compression or dry compression refrigerant types. Liquid suction heat exchangers only help the performance of wet compression refrigerant cycles. Description and explanations of these equipment functions follow.

3.9.1 Liquid Suction Heat Exchanger (LSHX)

A liquid suction heat exchanger is merely a liquid-to-vapor heat exchanger that uses the condensed liquid to superheat the compressor suction vapor, as described earlier. The condensate thereby subcools.

Thermodynamically, Figure 13 shows the added cooling effect, in the evaporator, of liquid suction heat exchange. Therefore, much less mass flow need circulate to provide any given level of cooling. The higher compressor discharge temperature, with its larger superheat, helps to avoid refrigerant liquefaction in the compressors. An optimum thermodynamic cycle for most wet compression fluids will often include as much liquid suction heat exchange as possible.

3.9.2 Economizer-Subcooler

The economizer-subcooler might be considered a direct-contact subcooling heat exchanger. In it, hot condensate flashes to a lower pressure. Some of the condensate vaporizes, absorbing its latent heat of vaporization. The remainder of the condensate, in direct contact with the vaporizing portion, remains a liquid, and subcools (i.e., compared to the condenser outlet temperature). The vapor enters the upper-stage compressor suction while the subcooled liquid flows to the evaporator, where it provides a greater cooling effect than it could at the condenser outlet temperature.

Thermodynamically, the economizer-subcooler performs two related functions. First, it allows the cycle to subcool its own condensate. Second, it allows a “staged” flashing. By flashing vapor in several steps, rather than one large step, some vapor may be routed back to the condenser via an appropriate intermediate compressor. This requires less total power

expenditure than sending all flashed vapor to the evaporator where one compressor, from a low pressure, must handle all the flashed vapor along with all directly evaporated liquid.

The subcooling in an economizer-subcooler allows more cooling effect per unit mass flow through the evaporator. Relatively little power is needed to overcome the small pressure rise back to the condenser, yielding a net positive gain in cycle performance.

Finally, the saturated vapor exiting the economizer-subcooler mixes with the still-superheated discharge gas leaving the intercooler. By simple mixing, de-superheating occurs, reducing high stage compressor work and discharge temperature.

3.9.3 Intercooler

An intercooler is a heat exchanger which rejects heat from low stage compressor discharge gas to a suitable lower temperature sink, external to the refrigerant cycle. In this application, the thermal transport loop fluid provides a sink for desuperheating the low stage compressor discharge. Discharge gas from the compressors was assumed to be cooled to 390K with the condenser temperature being 385K and the thermal transport loop fluid being 382K.

Thermodynamically, an intercooler allows the cycle to reject heat at an overall lower average temperature, closer to the condenser temperature. The desuperheating costs nothing internal to the cycle except the minor pressure loss through a heat exchanger. Without intercooling, upper stage compressor discharge temperatures would skyrocket. Intercooling also reduces the upper stage power input, since more mass moves for the same volumetric flow and pressure rise.

Dry Compression Fluid Cycle Optimization

Referring back to Figure 10 shows that the dry compression refrigerants depart from the Carnot ideal primarily due to a high compressor discharge temperature with large superheating. Compressor staging reduces the overall level of superheat, bringing the cycle closer in line to the Carnot ideal. Multiple compressors allow the “staged flashing” and subcooling of the

Figure 16 schematically shows a three-stage refrigeration system for a dry compression fluid

3.9.4 Direct Injection

Both figures indicate one new cycle modification, liquid injection. The direct injection of liquid refrigerant from a higher pressure source can fully desuperheat



The diagram is a Temperature-Entropy (T-s) plot. The vertical axis is labeled 'TEMPERATURE' and the horizontal axis is labeled 'ENTROPY'. A horizontal dashed line represents the condensing temperature, labeled T_{desup} . The cycle consists of the following components and processes:

- EVAPORATOR:** The process starts at the bottom left, moving horizontally to the right.
- FIRST STAGE ECONOMIZER-SUBCOOLER:** The refrigerant moves horizontally to the right, then diagonally up and to the left.
- EXP. VALVE:** A vertical dashed line indicates the expansion process from the first stage economizer-subcooler to the evaporator.
- SECOND STAGE ECONOMIZER-SUBCOOLER:** The refrigerant moves horizontally to the right, then diagonally up and to the left.
- EXP. VALVE:** A vertical dashed line indicates the expansion process from the second stage economizer-subcooler to the first stage economizer-subcooler.
- LIQUID INJECTION:** A horizontal line from the condenser to the second stage economizer-subcooler represents the injection of liquid refrigerant.
- CONDENSER:** The refrigerant moves horizontally to the right at the T_{desup} level.
- EXP. VALVE:** A vertical dashed line indicates the expansion process from the condenser to the second stage economizer-subcooler.
- THIRD STAGE COMPRESSOR:** The refrigerant moves diagonally up and to the right.
- INTERCOOL TO BUS:** A horizontal line from the third stage compressor to the second stage compressor represents the intercooling process.
- SECOND STAGE COMPRESSOR:** The refrigerant moves diagonally up and to the right.
- INTERCOOL TO BUS:** A horizontal line from the second stage compressor to the first stage compressor represents the intercooling process.
- FIRST STAGE COMPRESSOR:** The refrigerant moves diagonally up and to the right.
- INTERCOOL TO BUS:** A horizontal line from the first stage compressor to the evaporator represents the intercooling process.

A dashed line outlines the saturation dome, with the condenser operating in the subcooled liquid region and the evaporator operating in the superheated vapor region.

235 M94 013-8

compressor inlet gas. The liquid flashes and cools by direct contact vaporization. Commercially, present-day compressors use this method for compressor protection as the cooling keeps discharge temperatures within manufacturer's desired limits. With most standard refrigerants, however, liquid injection generally creates a net thermodynamic penalty.

However, with refrigerants exhibiting strong dry compression characteristics, liquid injection creates a net COP gain. Sacrificing a small amount of liquid prevents high discharge temperatures. Recall that high discharge temperatures are the major cause for dry compression fluid departures from the Carnot ideal. Strong dry compression fluids often have a large latent heat compared to their sensible heat. Thus, a small liquid injection sacrifice goes a long way towards bringing the compressor discharge temperatures closer to the condenser temperature.

3.10 A Review of Cycle Optimization, Dry versus Wet Compression Fluids

In general, all refrigerants benefit from staging. Staging gives lower discharge temperatures and permits intercooling and the staged flashing and subcooling of the economizer-subcooler. Thermodynamically, these processes bring any cycle more into line with the Carnot ideal in two general ways:

1. An average temperature of heat rejection closer to the minimum possible, the condenser temperature.
2. Better use of the flashing vapor and a closer to reversible flashing process.

Dry compression and wet compression refrigerants differ greatly concerning the benefits of a liquid suction heat exchanger or of liquid injection:

1. Dry Compression fluids: Obtain NET thermodynamic *benefit* from liquid injection.
2. Wet Compression fluids: Obtain NET thermodynamic *benefit* from liquid suction heat exchange.

These simple rules provide a practical definition for classifying dry compression and wet compression fluids. This quick classification scheme suffices for the first order choice of optimum cycle configurations, although borderline fluids may be technically classified incorrectly.

In actual practice, a refrigerant cycle for either type of refrigerant may employ either liquid suction heat exchange or liquid injection. Although liquid injection for a strongly wet compression fluid hurts COP, a designer may accept the COP degradation to obtain lower compressor operating temperatures for equipment reliability.

Similarly, liquid suction heat exchange for a strongly dry compression fluid gives a net COP loss, but other design considerations may dictate a liquid suction heat exchanger. For example, in supermarket applications vapor leaving the evaporator often travels a long distance to the compressor. Frequently, it picks up "junk heat" from the surroundings, superheating a large amount before reaching the compressor. Liquid suction heat exchange at least obtains the benefit of subcooling at the evaporator inlet which is better than allowing superheat at the outlet without obtaining any benefit.

3.11 Cascaded Refrigeration Cycles

A cascaded system places two independent cycles, each with its own refrigerant, one on top of the other. The two cycles require an intermediate condenser/evaporator. That is, the bottom cycle's condenser rejects heat to the top cycle's evaporator.

A cascade offers the advantage of moderate pressures and easy-to-work-with specific volumes at all points in the cycle. A cascade may ease the work of compressor designers and may not require multistaging within each cycle. With a cascade, one need not try to find a single refrigerant and complex cycle to meet the difficult demands of lifting heat from 275K to 383K. For a cascaded cycle one must find two refrigerants to work together, one suited for low temperatures and one suited for high temperatures. The bottom cycle can therefore use a volatile refrigerant such as ammonia or

HFC-134, and the top cycle can use a less volatile, lower pressure refrigerant such as HCFC-123a or water.

A cascade has at least two disadvantages. One is the additional weight of an inter-cycle heat exchanger and the other is the temperature lift added by the differential across this heat exchanger. Simplified cycles, with fewer intra-cycle heat exchangers, and better fluid performance may offset these disadvantages somewhat, though results show that other single refrigerant cycles can match these performance gains without the disadvantages.

3.12 Other Considerations

This section explains some of the reasons for the different refrigerant characteristics and behaviors. The chemical stability needed for ozone safety inherently conflicts with a fluid's refrigerant quality (4). Chemically stable molecules, such as perfluorinated carbons (FCs) act like "hard spheres" and have no loosely bonded radical groups or atoms, such as hydrogen or chlorine. Less stable molecules have loosely bonded radical groups or atoms hanging to the side, and are available to react, break down, or absorb energy, such as for latent heat.

As a detriment to their refrigerant qualities, these chemically stable molecules offer little energy-absorption locations. A "hanging" atom offers polar effects between molecules and other ways of absorbing energy. These effects lead to "sponge-ball" molecular behavior, large latent heat per unit mass and higher critical temperatures. Note that Trouton's rule remains unaffected: the ratio of molar latent heat to absolute critical temperature stays approximately constant.

Thus, the ongoing national search for ozone-safe refrigerants will not likely uncover better refrigerants than the CFCs. HFCs provide performance improvement over pure FCs, and for more moderate refrigeration cycles can come close to CFC performance. This is particularly true with equipment to improve the thermodynamics of the standard refrigeration cycles. Under the extreme conditions required by the lunar base heat pump, however, HFCs offer candidates unlikely to match CFC-11

performance. Note that one of the best new "green" refrigerants, HCFC-123, still has some chlorine.

Some more "extreme" refrigerants were considered, such as the hydro-fluorinated-ethers (HFE). These were researched for availability only as they are completely unproved as refrigerants, and are often toxic. Flammable and/or corrosive fluids such as methyl or ethyl amine, methanol, ethanol, and pentane were also evaluated. These chemicals have the hanging atoms or radical groups to give good refrigerant properties, and the right range of critical temperatures. However, their disadvantages suggest caution.

The following attempts to explain the causes of the wet and dry compression refrigerant behaviors. Heavier, larger molecules move the behavior toward wet compression because large molecules create a large molar heat capacity (3,4). The numerous chemical bonds and the atomic mass of a large molecule offer significant thermal energy storage. Added bonds add degrees of freedom. Bonds may oscillate, rotate, or even bend. Each of these "bond-distortions" add energy-absorbing ability to a molecule, thus molar heat capacity increases. Large molar heat capacity means minimal increase in compressor discharge temperature, since the fluid can absorb a lot of heat without raising its temperature. Large molar liquid heat capacity, especially when compared to the latent heat, means a lot of flash gas loss. In other words, during the flashing process, much vapor must evaporate to subcool the remaining liquid, hence the large throttling loss. Dry compression fluids, on the other hand, superheat badly during compression due to their relatively low molar heat capacity. During flashing, however, they require very little vaporization to absorb, via latent heat, the necessary energy to subcool the remaining liquid.

All chemically stable, nontoxic, and nonflammable refrigerant compounds start as a fluorinated carbon compound (3). These large molecules create strongly wet compression fluid types. Strongly wet compression refrigerant behavior deteriorates COP by limiting the cooling effect in the evaporator. Liquid suction heat exchangers cannot completely overcome this limitation, so chemists replace some fluorine

atoms with hydrogen atoms to lighten the molecule and give it a weaker wet compression behavior. The hydrogen, however, adds some chemical instability and flammability. Once again, this explanation makes clear another reason why R-123a performs reasonably well. It behaves as a weak wet compression fluid.

Modern chemistry isn't likely to deliver any dramatic improvements over the refrigerants analyzed here (2-4). The search for a nontoxic, nonflammable, chemically stable, noncorrosive, yet thermodynamically efficient refrigerant consists of refinements in fluid property selection and careful cycle design. Accepting toxic or flammable refrigerants does offer possible performance improvements.

3.13 Refrigerant and Thermodynamic Cycle Selection Results

Tables 6 through 9 summarize the results of this work with refrigerant cycles and fluids for the lunar application which was the basis of the refrigerant selection. The foregoing discussion was intended to give more meaning to these tabulated numerical results. The left-hand column lists the refrigerants considered. The next two columns list the atmospheric boiling temperature and the critical temperature, respectively. The boiling temperature gives a qualitative indication of pressure and specific volume at the evaporator temperature of 275K. High boiling points mean low pressure, large specific volume, and large equipment at the evaporator end of the cycle. The critical temperature gives a pass-fail signal of whether a fluid can operate in a vapor-compression cycle with a 385K condenser temperature. Critical temperatures below 385K fail without further evaluation. Critical temperatures above, but close to, 385K usually indicate unlikely fluid candidates. Only a wide liquid-vapor dome, such as that possessed by ammonia, can overcome this handicap.

To the right of this basic refrigerant information, more columns list calculated cycle performance. These COPs were calculated from accurate refrigerant properties, usually computer-generated, assuming a 65 percent compressor performance. Other factors such as achievable compression ratio and system pressure drops were ignored to simplify calculations for this step of the selection process.

3.13.1 Wet Compression Refrigerants, Single-Stage Cycle

Table 6 includes the results of single-stage performance calculations of wet or nearly wet compression fluids (i.e., CFC-11). Note that the work was performed for two different cycles. One cycle assumed very effective liquid suction heat exchange where the Liquid Suction Heat Exchanger Temperature Difference (LSHX TD) equals 5.5K. This means that the vapor superheats to within 5.5K of condenser outlet temperature. The second cycle assumed less effective heat exchange with an LSHX TD equal to 28K, vapor superheats to within 28K of the condenser outlet temperature. Varying the LSHX TD shows the sensitivity of the cycle to the LSHX effectiveness.

The high discharge temperatures for these cycles indicate that no practical single-stage design will likely be acceptable. This analysis proves a useful filter to eliminate many refrigerants. Specifically, cycles which show a low single-stage COP were eliminated from further consideration. Multistaging improves the COP somewhat, but mostly acts to lower discharge compressor temperatures. Other refrigerants with reasonable single-stage COPs, but which show undue sensitivity to liquid suction heat exchange, were also eliminated.

Some wet compression fluids, such as the HFEs (Hydro-Fluorinated-Ethers) are research chemicals, noncommercial, hard to manufacture, very hard to obtain and have unknown toxicology. They hold some promise (high latent heat, high critical temperatures) of giving good COPs.

Preliminary cycle calculations were performed on ethers, but did not yield extraordinary COPs. These refrigerants were not pursued because they have difficulties which require considerable development. This necessary extra work would seemingly push their practical use far into the future.

3.13.2 Dry Compression and Cascade Cycle Topping Fluids

Table 7 is a short list that only shows the boiling temperature and critical temperature of the few dry compression refrigerants found and of some candidate pure topping fluids.

Table 6. Performance Summary: Single-Stage, Wet Compression Refrigerants

All temperatures in degrees K; all cycles use Overall Compressor Efficiency = 0.65 to include motor

Refrigerant	T _{Boil} (°K)	T _{Crit} (°K)	Wet (or nearly so) Compression Refrigerants - One-Stage with LSHX					
			LSHX TD = 5.5°K			LSHX TD = 28°K		
			COP	% Carnot	T _{dis} (°K)	COP	% Carnot	T _{dis} (°K)
CFC-11	297	471	1.17	47	576			
CFC-113	321	487	1.19	48	519			
CFC-114	277	419						
HCFC-123	301	457	1.07	43	434	0.72	29	410
HCFC-123a	303	463	1.12	45	525	1.04	42	499
HCFC-124	261	395	0.74	30	509	0.65	26	486
HCFC-125	225	339	Fail	-	-	Fail	-	-
HFC-134	254	392	0.72	28	529	0.65	26	505
HFC-134a	246	374	Fail	-	-	Fail	-	-
HFC-143a	225	346	Fail	-	-	Fail	-	-
AZ-20	221	346	Fail	-	-	Fail	-	-
AZ-50	227	344	Fail	-	-	Fail	-	-
Perfluorocarbons								
C3F8 (=R-218)		345	Fail	-	-	Fail	-	-
C4F8 (=RC-318)		388	0.43	17	-	-	-	-
C4F-10	273	386	Fail	-	-	Fail	-	-
Butanes								
HFC-338ocb	301	434						
HFC-338eea	299	421						
n-Butane	273	425	1.13	45	497			
i-Butane	261	408	1.08	43	490			
Others								
E-134	279	420						
R-141b**		477	Flammable					
R-142b		410						
E-143*	303	460	Flammable					
R-143	277	430						
R-152**	304	476	Flammable					
R-218		345	Fail	-	-			
E-227ca	270	388						
HCFC-235ca	301	444						
R-236ca	278	412						
R-236cb	272	403						
R-236ea	280	414						
R-236fa	272	404						
E-245cb*	307	458	Little data					
HFC-245ca*	298	451	Falls 1 to 2% behind HCFC-123 in normal refrigerant cycles; flammable in humid air					
R-245fa	289	431						
E-254cb*	310	463	Little data	17				
RC-318		388	0.43					

*Marginal probable performance.

**Worth checking.

Otherwise, unmarked and un-rated fluids are unlikely performers.

Table 7. Performance Summary: Dry Compression and Topping Refrigerants

Refrigerant	T _{Boil} (°K)	T _{Crit} (°K)	Comments
HCFC-22	233	369	Fail
Ammonia	240	405	See multistage results
SO ₂	264	430	See multistage results

Exclusively Topping Refrigerants	T _{Boil} (°K)	T _{Crit} (°K)	Comments
Water	373	647	Dry compression
Cyclo-Hexane	354	554	Wet compression
Perfluorocarbons			
FC-72	328	451	Wet compression
FC-75	375	500	Wet compression

Knowing that excessive discharge temperatures would occur, dry compression fluids in single-stage cycles were not carefully evaluated. Quick single-stage estimates showed whether the fluids held any interest for multistage evaluation. More detailed two- and three-stage cycle calculations, shown in Table 8, brought compressor discharge temperatures down to reasonable levels.

3.13.3 Multiple Stage Refrigerant Cycles

Table 8 is self-explanatory. The leading contender was CFC-11, with the highest performance. There is also available a great deal of industry equipment and safety experience with CFC-11. However, it is targeted for phase out and replacement by its "green" refrigerant counterpart, HCFC-123. HCFC-123 is the highest performing commercially available HCFC for this application. However, it only ranked number 7 of the seven leading candidates in single-refrigerant cycle performance and is below that of a water-ammonia cascaded cycle.

Several of the top performing fluids listed in Table 8 were ruled out for reasons other than performance. HCFC-123a performed nearly as well as CFC-11, is a "green" refrigerant and had a higher performance than HCFC-123. However, it is not commercially available and would create unacceptable logistics problems in obtaining and maintaining an adequate supply.

One highly flammable refrigerant, n-Butane, performed well but was ruled out because of the safety concerns associated with its flammability. CFC-113 was ruled out for similar reasons to CFC-11, environmental impact from operating the ground-based prototype. Ammonia and sulfur dioxide were ruled out because of toxicity.

When reviewing this data, note discharge temperatures and, for wet compression fluids, sensitivity to changes in liquid suction heat exchanger performance. Also note that the calculations for the marked results account for compression ratios that are achievable by existing compressor technology. They also account for estimated system pressure drops. Hence, these calculations represent realistically obtainable heat pump results.

3.13.4 Cascaded Cycles

In Table 9 a 5.5K difference between the bottom cycle condenser and the top cycle evaporator (Inter-cycle TD = 5.5K) was assumed. The close-to-optimum interstage temperature appears to be 336K. That is, the bottom cycle condenser runs at 338K, rejecting heat to the top cycle evaporator at 333K.

In all cascades shown, the bottom cycle has an intercooler to lower compressor discharge temperature to 390K using the thermal transport loop fluid. Every bit of heat dumped BEFORE

Table 8. Performance Summary: Promising Multistage Refrigerant Cycles

Refrigerant	T _{Boil} (K)	T _{Crit} (K)	Wet Compression Refrigerants Subcooler, Intercooler, LSHX						
			Two-Stage			Three-Stage			
			COP	% Carnot	T _{int}	T _{dis} (K)	COP	% Carnot	T _{int} T _{dis} (K)
CFC-11*	297	471	1.38	55	350	429/481	**1.49	56	350/317 419/416/381
HCFC-123a	303	463	1.28	51	351	414/451	**1.30	52	350/311 405/382/354
n-Butane	273	425	1.30	52	350	409/431			
CFC-113	321	487					**1.30	52	361/333 403/399/397
HCFC-123	301	457	0.95 lunar 1.06 SIRF	**38 lunar 43 SIRF	369	390/404			
Dry Compression Refrigerants Subcooler, Intercooler, Liquid Injection									
Refrigerant	T _{Boil} (K)	T _{Crit} (K)	Two-Stage			Three-Stage			
			COP	% Carnot	T _{int}	T _{dis} (K)	COP	% Carnot	T _{int} T _{dis} (K)
			COP	% Carnot	T _{int}	T _{dis} (K)	COP	% Carnot	T _{int} T _{dis} (K)
Ammonia	240	405	1.19	48	335	446/473	**1.24	50	356/317 413/416
Sulphur Dioxide	264	430	1.24	50	333	444/433			
*Rated at 378K radiator temperature. **Account for achievable compression ratios and system pressure drops.									

Table 9. Performance Summary: Cascades

Top	Bottom	Wet Compression CASCADE Stacked Single-Stage LSHX Cycles, Bottom Cycle with Bus Desuperheat					
		LSHX TD = 5.5K			LSHX TD = 28K		
		COP	% Carnot	T _{dis} (K)	COP	% Carnot	T _{dis}
HCFC-123a T _{cond} = 385K T _{evap} = 335K	HFC-134 T _{cond} = 340K T _{evap} = 275K	1.12	45	432/430	0.99	40	406/414
		Dry Compression CASCADE Stacked Cycles with Bottom Cycle Desuperheat to Bus					
Two-Stage Water T _{cond} = 385K T _{int} = 373K T _{evap} = 333K	Single-Stage Ammonia T _{cond} = 339K T _{evap} = 275K	COP	% Carnot	T _{dis} (K)			
		1.25	50	430/579/478			
		Mixed CASCADES Appropriate Cycles, Bottom Cycle with Bus Desuperheat					
Two-Stage HCFC-123a T _{cond} = 385K T _{int} = 371K T _{evap} = 333K	Single-Stage Ammonia T _{cond} = 339K T _{evap} = 275K	LSHX TD = 5.5K			LSHX TD = 28K		
		COP	% Carnot	T _{dis} (K)	COP	% Carnot	T _{dis}
		1.20	48	407/478	1.15	46	399/478

Top	Bottom	Mixed CASCADES Appropriate Cycles, Bottom Cycle with Bus Desuperheat					
		LSHX TD = 5.5K			LSHX TD = 28K		
		COP	% Carnot	T _{dis} (K)	COP	% Carnot	T _{dis}
HCFC-123a T _{cond} = 385K T _{evap} = 333K	Ammonia T _{cond} = 339K T _{evap} = 275K	1.18	47	434/478	1.13	45	412/478
FC-72 T _{cond} = 385K T _{evap} = 333K	Ammonia T _{cond} = 339K T _{evap} = 275K	1.04	42	478			
Cyclohexane T _{cond} = 385K T _{evap} = 333K	Ammonia T _{cond} = 339K T _{evap} = 275K	1.22	49				
Two-Stage Water T _{cond} = 385K T _{int} = 373K T _{evap} = 333K	HCFC-123a T _{cond} = 339K T _{evap} = 275K	1.27	51	430/579/524			
HCFC-123 T _{cond} = 385K T _{evap} = 334K	HFC-134a T _{cond} = 336K T _{evap} = 275K	1.09	43	399/406			

reaching the top cycle evaporator boosts overall cascade COP significantly. For this reason, a cascaded system actually favors using a single-stage bottom cycle. A single-stage bottom cycle has slightly lower bottom COP than a two-stage bottom cycle. However, the large heat rejection of the single-stage bottom cycle intercooler unloads the top cycle and the overall cascade COP improves.

No overall COP benefit was obtained by cascading the Lunar Base heat pump. The moderate operating pressures and vapor densities and the simple single-stage bottom cycles, however, may offer some weight and reliability advantages.

All cascades with water on the top cycle would require high volumetric flow rate compressors and generally large equipment to handle the high specific volume. Water rated as a refrigerant with superlative refrigerant qualities (high latent heat, high critical temperature) for a cascaded

cycle. However, it requires overcoming many compressor difficulties. The cascaded cycles using water did not have high enough COPs to warrant overcoming these difficulties. The improvement offered by triple-staging the water topping cycle does not warrant the additional complexity and associated development required.

3.14 Refrigerant and Thermodynamic Cycle Selection Conclusions

As shown in Tables 10 and 11, the leading contender was CFC-11, with the highest performance. There is also available a great deal of industry equipment and safety experience with CFC-11. However, it is targeted for phase out and replacement by its "green" refrigerant counterpart, HCFC-123. HCFC-123 is the highest performing commercially available HCFC for this application and ranked a close number 3 overall. Ammonia was chosen due to toxicity.

Table 10. Single Refrigerant Cycles

Refrigerant	Configuration	% Carnot COP
CFC-11	Three-stage, base	56
	Two-stage, SIRC	55
Ammonia	Three-stage, base	50
HCFC-123	Two-stage, base	50
	Two-stage, SIRC	40

Table 11. Cascaded Cycles

Upper Stage Refrigerant	Configuration	Lower Stage Refrigerant	COP	% Carnot
Water	Two-stage	HCFC-123a	1.27	51
Water	Two-stage	Ammonia	1.25	50
HCFC-123a	Two-stage	Ammonia	1.20	48

4. COMPRESSOR SELECTION

4.1 Selection Process

There are several requirements and criteria for the selection of compressors for the lunar mission heat pumps:

- *Size* and size range to satisfy the base station at 25 kW heat load, and the lunar lander at 5 kW, preferably using the same or similar compressors in order to facilitate development.
- *Redundancy* in the system so that 80 percent capacity (20 kW) remains after one failure, and 40 percent after two failures.
- *Control* capability to allow operating at variable loads to minimize power usage during the morning and evening of the lunar day. This is needed when the radiator and condenser temperatures are reduced, and when the thermal load from the lander or base is independently reduced.
- *Efficiency* maximized in order to minimize the total system mass, in which the mass of the power supply system is the largest and most variable component.
- *Life* approaching 30 years with a duty cycle of 4000 hr/year (off at night).
- *Flexibility* to handle somewhat different refrigerants and heat pump cycles in order to accommodate cycle development and the unpredictable availability of certain refrigerants.

All of these criteria are fairly obvious except for control and flexibility. These criteria are linked because of two independent effects, reduced mass flow and reduced pressure ratio. These effects can occur at the same time. Reduced mass flow occurs when the demanded

cooling load becomes lower than the design load at any time during the day, while the source and sink temperatures remain as given. Consequently, the heat pump system must reduce evaporator mass flow without reducing the temperature (pressure) lift of the compressors. Reduced pressure occurs when, for a given load, the radiator and condenser temperatures reduce as the sun drops toward the horizon and the effective sink temperature of the radiator drops. Consequently, the temperature (pressure) lift of the compressors reduces while the mass flow remains constant.

Initial evaluation of compressor types, for a particular application, can be made on the basis of specific speed and specific diameter. This correlation was developed for selecting and matching turbines and compressors for aerospace rocket motor applications. In any pump/compressor application, the flow and head (work/mass) are the requirements, the shaft speed is a given or selected parameter, and the size (diameter) of the compressor (rotor) is the penalty to be accepted. Alternatives are the compressor type and the number of stages used to accomplish the total head. Figure 18, adapted from Balje (5) shows the general variation of efficiency with specific speed and diameter for a wide range of different compressor types. Turbo (centrifugal) machines and rotary (volumetric) machines are shown. Although the efficiency range of piston types is not given, their usual range of specific speed is near one. Figure 18 shows that centrifugal and rotary machines can have comparable efficiency and rotor size, although at quite different speed levels for the same flow and head per stage. The two different efficiency maps for rotary machines represent different ratios of rotor clearance to rotor diameter. The points indicated are for specific examples of refrigeration machines: centrifugal, screw, and rolling piston types developed for aerospace applications by Allied,

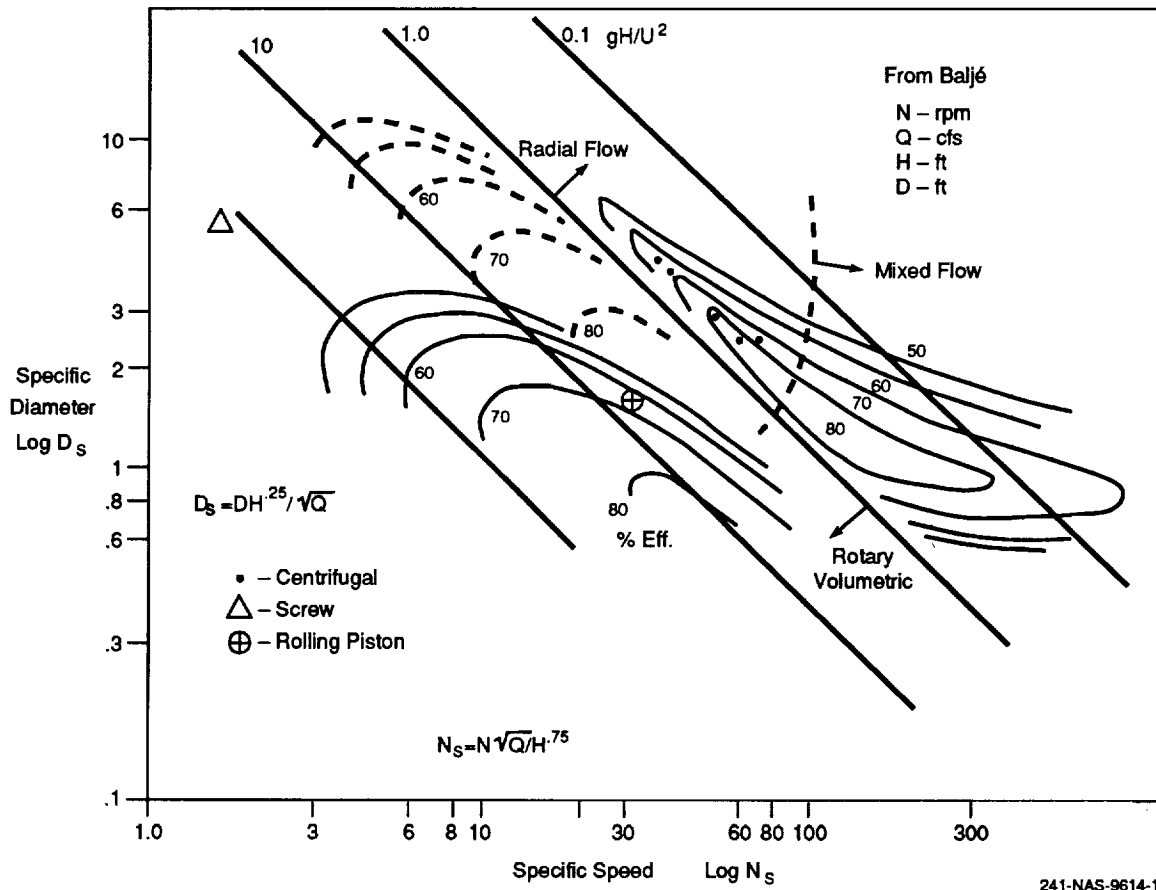


Figure 18. Variation of Efficiency of Compressors with Specific Speed and Diameter

Fairchild, and Sundstrand, respectively. Exceptions are the points at low efficiency for centrifugals, which are projected for subsequent stages on a single shaft, to be discussed.

Motor size, efficiency, and system controllability must be considered in the system design as well as compressor speed, size, and efficiency. In general, motor size (mass) decreases almost directly as speed increases, but efficiency usually suffers somewhat. Rotor windage power, iron hysteresis, and iron eddy current losses all increase as speed increases for the same net power. This assumes design parameters such as flux and current densities are held constant. Copper resistive losses may decrease or increase slightly when scaling the motor design for higher speed. This depends on the ability to cool the windings, which becomes more difficult as motor size decreases.

Speed control (and the probability of using a photovoltaic DC power supply) requires the use of synthesized variable frequency. The most compact motors are electronically commutated DC (ECDC), or "brushless" DC. Synthesis of multiphase variable frequency power for efficient motors becomes more difficult at speeds much over 25 krpm. Although speeds of 250 krpm or more have been achieved.

The choice of compressor types was between centrifugal and rotary machines, while the selected refrigerants are R-11, based on performance, and R-123a based on future availability. Compressors that could use these refrigerants interchangeably was preferred. Initial analysis using the method of Balje, as well as manufacturers' data, showed that the speed of centrifugal compressors would be above 70 krpm. The rotary compressors would all run

below 40 krpm. Only the first stage centrifugal for the lunar base would be run at 70 krpm. Appropriate speeds for later stages of the base heat pump, and any stage for the lunar lander, would run higher, up to 200 krpm.

Figures 19 and 20 show the typical characteristic performance maps, in non-dimensional form, applying to all sizes of centrifugal and rotary screw compressors. Both types have good efficiency at pressure ratios between 2 and 4. This fits well with the three stage optimum cycle. Centrifugal compressors appear to have slightly higher efficiency, but this is probably not so when the windage losses are included for the bearings and the motor. These losses are relatively large for the small compressor rotor diameters required. Also, in our case the absolute size of the compressor will be quite small, less than 7 cm, making good aerodynamics harder to achieve (due to difficulties of fabrication and Reynolds' number). Although detailed design comparison was not within our scope, we estimated that the combined motor and compressor efficiency of centrifugals would be lower than that of screw machines.

The performance maps in Figures 19 and 20 show that the screw machine has a much broader range for good efficiency as mass flow and pressure ratio vary during system operation. Flow and pressure can vary independently within an "island" of good efficiency, and compressor stall is not a problem. Neither fact is true for centrifugal compressors. Control flexibility is especially important when multiple compressors are used for redundancy. The best plan to provide the required 80 percent capacity after one failure and 40 percent capacity after two failures is to install three compressors per stage and to run either two or one. This provides 100 percent and 50 percent capacity with one and two failures while minimizing the size and number of installed compressors. However, centrifugal compressors cannot be run in parallel except in their regimes of negative pressure/flow rate change, or "slope." This is problematic with respect to efficiency and control.

For all of the reasons discussed, Foster-Miller selected rotary, positive displacement compressors for both the lunar base and the lander.

4.2 Sizing of Rotary Compressors

Only a small number of models of rotary refrigerant compressors exist in the aerospace market. The designs are not basically different from rotary compressors for commercial refrigeration, but the aerospace units are smaller, higher speed, flight qualified and much lighter for the same cooling capacity. One can expect that the motors, bearings, and housings will be specialized for the lunar missions, but the basic rotor geometry will remain the same. The lunar base and lander systems can employ rotor sizes that presently exist. New intermediate sizes could be considered in the ultimate program optimization. For this preliminary design program we elected to use data on screw compressors from Fairchild Corporation, and on a rolling piston compressor by Sundstrand. Other aerospace rotary compressors exist that might be suitable. A brief review was published by researchers at Wright-Patterson AFB (6).

4.3 Lunar Base Compressors

The lunar base design comprises three stages having three screw compressors per stage. At any time only a maximum of two compressors per stage are run, 12.5 kW thermal capacity each. Reduced speed produces reduced capacity, and reduced radiator temperature reduces the operating pressure ratio. Existing screw compressors have 54, 40 or 30 mm rotor diameters for different capacity ranges. Figure 21 shows an exploded view of a typical model, the Fairchild 54 mm. In general for all these models, the installed power and case size are larger than needed for our purposes because they were designed for R-12, a higher pressure refrigerant than R-11 or R-123. Consequently, a lunar design based on the same compressors could be smaller and lighter. Table 12 describes the design parameters for all three stages, the power and weight of existing compressor and motor assemblies, and the projected mass of this basic model after the motor and housing are sized for the lunar mission.

Figure 21 is an exploded view of the 54 mm Fairchild screw compressor as it now exists, and Figure 19 is the actual performance map, non-dimensional, of all their screw compressors using R-11.

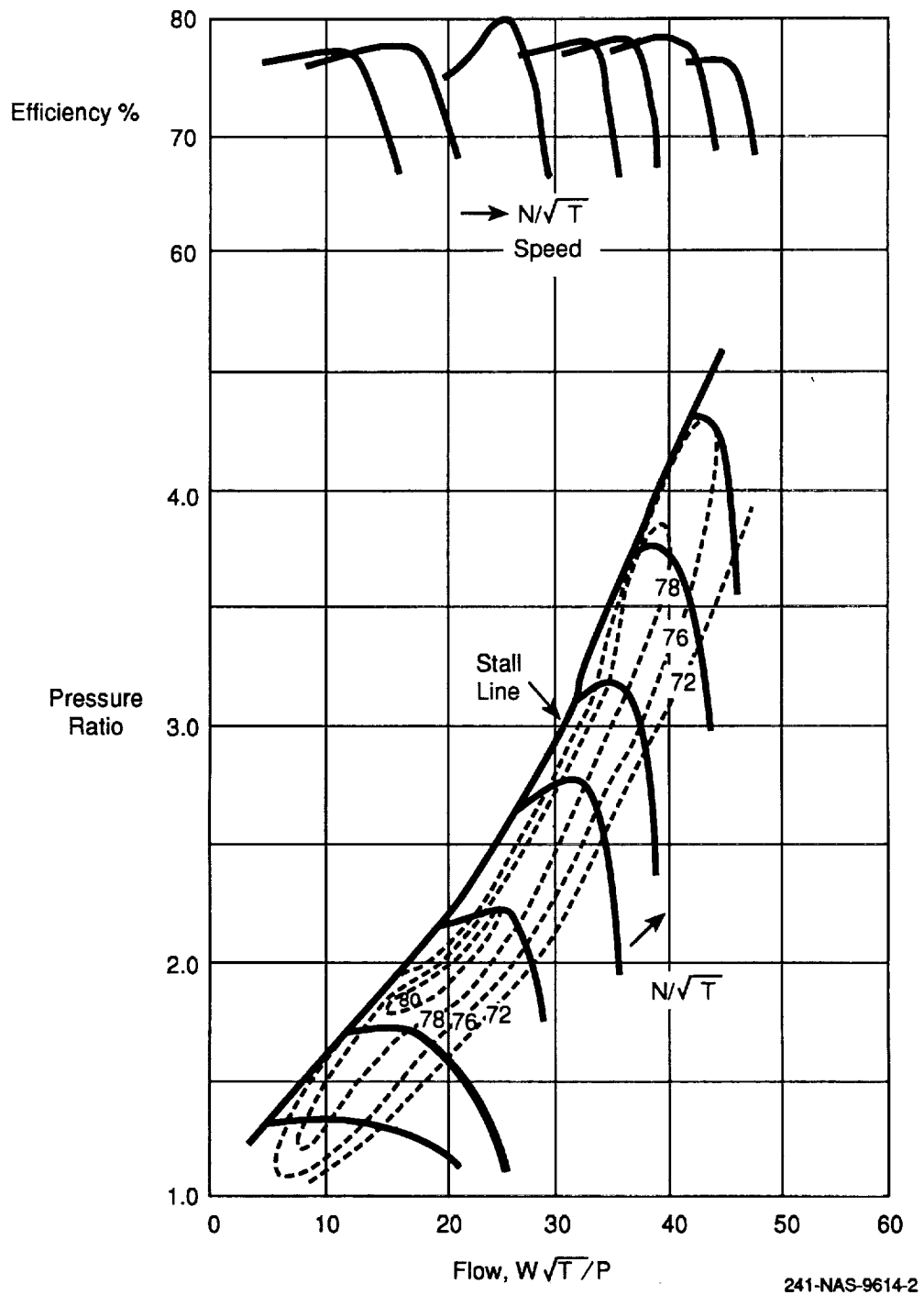


Figure 19. Typical Performance of a Centrifugal Compressor

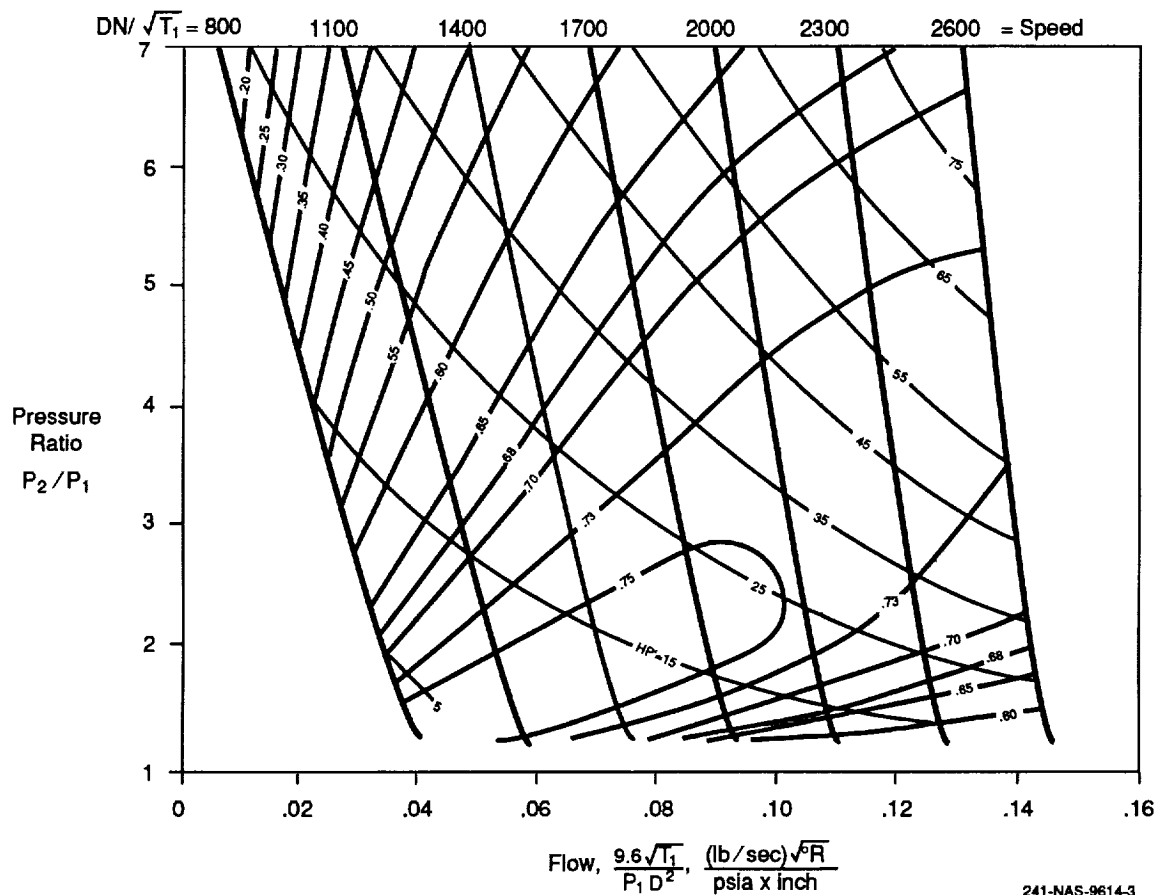


Figure 20. Performance of Fairchild Screw Compressors on R-11

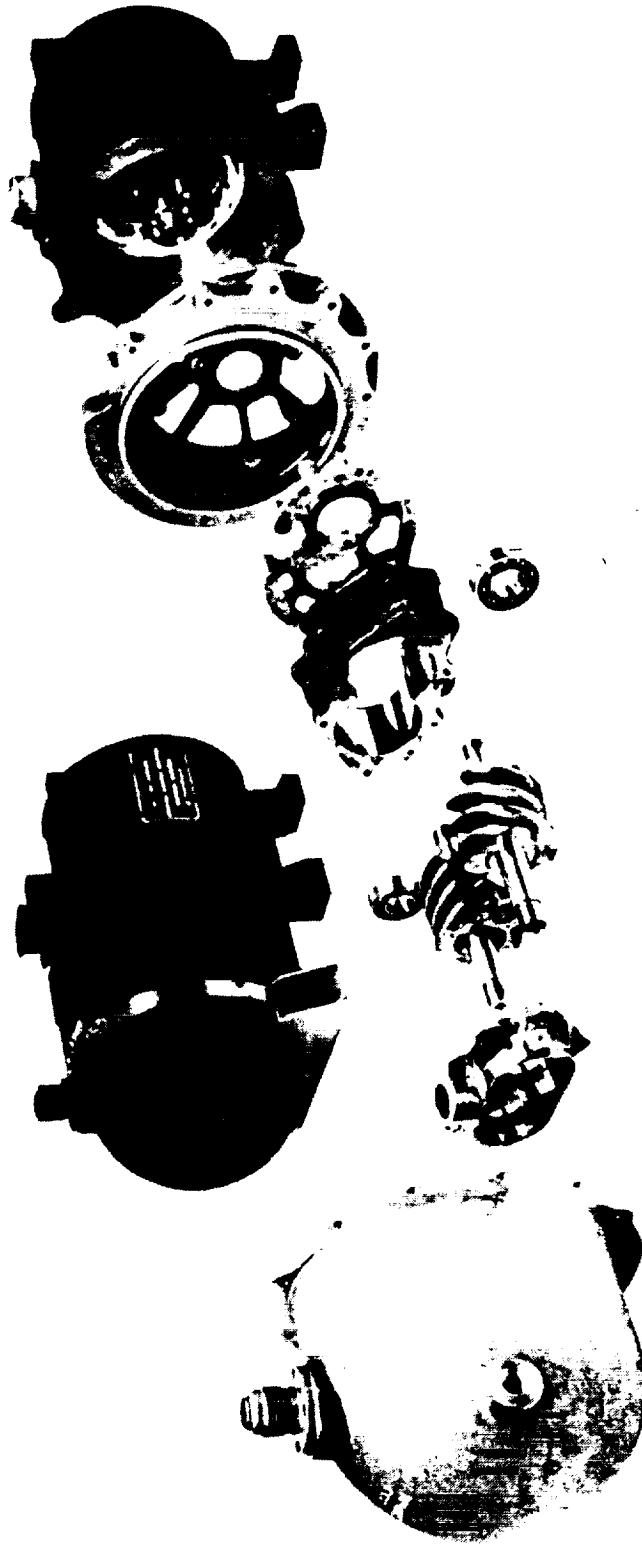
4.4 Lunar Lander Compressors

The lunar lander also requires three compressors per stage in order to meet redundancy requirements, but for simplicity and because smaller screw compressors are not available, only two stages are employed. The first stage uses screw compressors, while the second stage uses high-pressure rolling piston compressors. Figure 22 shows the operation of this type compressor in axial view, and Figure 23 is a cross-sectional view of the Sundstrand compressor sized for R-114 in the LANTIRN avionics pod cooling application. A smaller rolling piston compressor is used in the Pathfinder pod. Since generalized performance maps for R-11 and R-123a are not available, the optimum selection is problematic. At this time it is clear that running one compressor of LANTIRN size has adequate volume capacity

for 5 kW thermal capacity, second stage. Table 12 defines the design parameters for the second stage compressor set. Again one can expect that the unit size and mass will decrease when the appropriate motor and housing are developed.

4.5 Compressor Development for Lunar Mission

Although the preceding discussion shows that the existing screw and rotary compressors have satisfactory basic capacity, they have been designed for different refrigerants, power, and life cycles from those expected in the lunar missions. Resizing the motors and housings is straightforward. Using electronic speed control can maintain an optimum speed within the range where the existing rotors are structurally adequate. Since both screw and rotary type



07885

Figure 21. Exploded View of Fairchild Screw Compressor and Motor

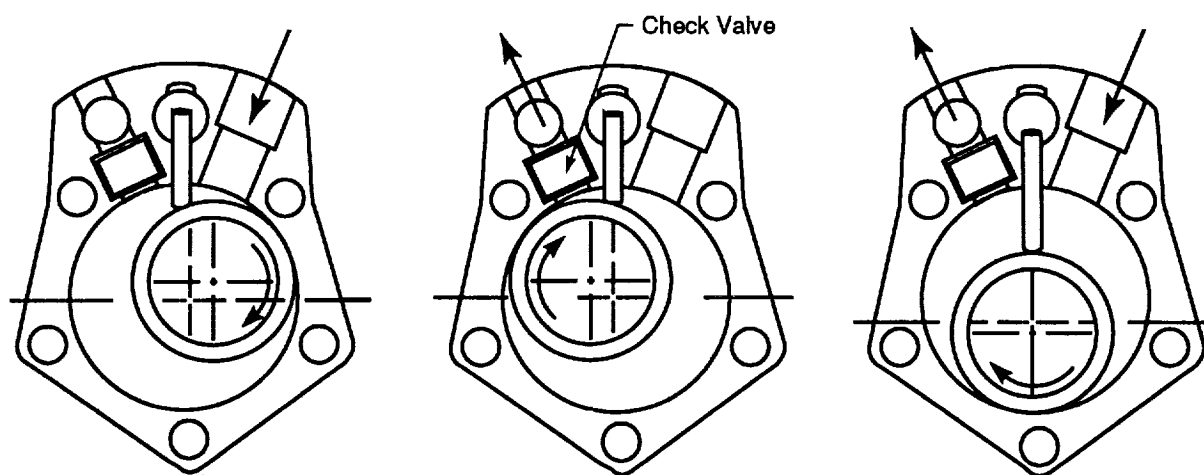
Table 12. Compressor Design Parameters for the Lunar Base and Lander

Design Parameters for 25 kW Lunar Base Compressors
Three Screw Compressors, per Stage Installed, Two Run per State

Stage	Pressure Ratio	Rotor Size (mm)	Dimensionless Flow $W\sqrt{T} / PD^2$	Speed (krpm)	Efficiency (Percent)	Existing		Projected		
						Power (kW)	Mass (kg)	Power (kW)	Mass (kg)	X3 (kg)
1	4.5	54	0.134	28.6	74	26	14.6	3.4	9	27
2	2.5	40	0.071	23.7	75	14	11.4	3.0	7	21
3	2.4	30	0.065	29.2	74	3.5	7.7	3.2	5	15

Design Parameters for 5 kW Lunar Lander Compressors
Three Screw Compressors, Run 2; Three Rotary Compressors, Run 1

Stage	Pressure Ratio	Rotor Size (mm)	Dimensionless Flow $W\sqrt{T} / PD^2$	Speed (krpm)	Efficiency (Percent)	Existing		Projected		
						Power (kW)	Mass (kg)	Power (kW)	Mass (kg)	X3 (kg)
1	5	30	0.087	37	71	3.5	7.7	0.7	5	15
2	5.4	57	NA	5.5	65/70	5.3	9.1	2.0	5	15



241-NAS-9614-4

Figure 22. Schematic of Rotary (Rolling Piston) Compressor Operation

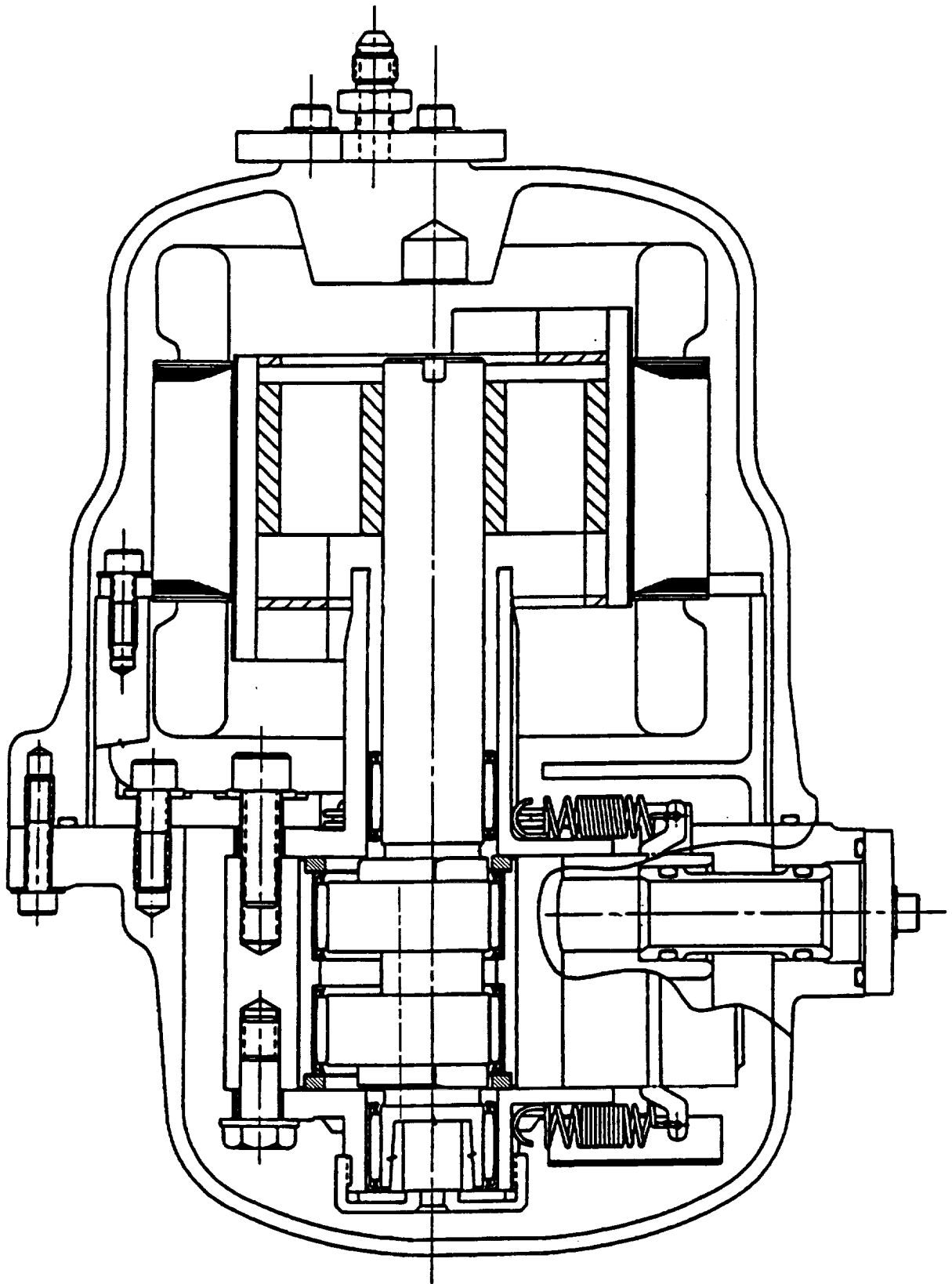


Figure 23. Schematic of Rotary (Rolling Piston) Compressor Operation

compressors are run with oil entrained in the vapor stream and flooding the clearances, the rotors can run for decades. Commercial units have shown this. Bearing design for very long life is the remaining design objective.

Commercial screw compressors are made with either rolling element bearings or fluid film bearings. Both can achieve very long life if well developed, but small compressors usually use the former, while large compressors, the latter (7). Full-film bearings have unlimited life in clean, hermetic systems. Rolling element bearings loaded to only one quarter of their usual high load capacity have predicted fatigue lives (90 percent reliability) of 30 years, 50 percent duty, in hermetic environments. With either type of bearing, lubrication control is the critical factor. Compressors will require oil separators downstream, and oil distribution from a sump to several points. Moon gravity, though lower than Earth's, is quite adequate for typical sump systems.

Most rolling piston compressors are small and cost-driven, so they employ journal bearings for shaft and rotor, as well as oil flooding of rotor/cylinder clearances. The Fairchild compressor initially selected has "needle" bearings and polymeric sealing members in some places. The most appropriate approach for the lunar missions remains to be proven, but residential rolling piston models have demonstrated decades of life during more severe cycling than is expected on the moon.

4.6 Compressors for the SIRF

The aerospace compressors selected initially for lunar base and lander missions are much too expensive for the scope of the SIRF program. However, the basic objective of the SIRF is to demonstrate the heat pump system (i.e., its

various components, interconnections, packaging, and control method and response). For this, the most important characteristics of any compressor are its parametric relationship between head, flow, and speed, and its requirements for lubrication and heat dissipation.

The *screw* compressor works by trapping low pressure vapor between meshing rotors, reducing the mesh-trapped volume during rotation to achieve some vapor compression, and then displacing the remaining mesh volume through a port into the high pressure vapor receiver. Exactly this process occurs in common commercial *scroll* compressors, except that the mesh geometry is topologically different. Both types are usually run with sufficient oil entrainment in the inlet to seal the mesh clearances, and they have comparable efficiencies. They do run at different speeds for the same cooling capacity, however. Scroll compressors for 5 kW capacity running on 60 Hz power are quite reliable and inexpensive. With a variable frequency power supply their capacity can be varied in the same manner as planned for lunar screw compressors. *Commercial scroll compressors are recommended for the first stage of the SIRF compressor set.*

Rolling piston compressors that run on 60 Hz power and have the required displacement for the second stage of the SIRF are available commercially. They are reliably used in residential heat pumping and similar applications. They can also be controlled using variable frequency, as mentioned for screw compressors. The only question concerning their use for the second stage of the SIRF is whether they will withstand operation at the high discharge temperature associated with the simulated high condensing temperature of the SIRF. This problem can be overcome using appropriate oil and additional cooling for the motor stator.

5. LUBRICATION/OIL MANAGEMENT AND CONTROL

The 1/6g gravitational field on the lunar surface is adequate to use terrestrial technology. This technology consists of an oil sump in the compressor with direct feed to the critical areas such as bearings and rotor or scroll surfaces. The oil is then carried over in the discharge gas where it is centrifugally separated by cyclone separators. Separated oil is returned to the sump by both the pressure differential between the gas discharge and sump and by gravity. The oil is then re-distributed.

Oil separation in the cyclone separator does not have to be 100 percent complete because the gas velocity, 200 ft/min minimum, is adequate to keep the oil entrained for eventual return to the compressor inlet. Return lines from anticipated system collection points to the oil sump are used to prevent oil buildup in the system and eventual starvation of the compressors. The critical areas of the system are found in the vertical rises.

6. HEAT EXCHANGER SELECTION

The heat pump system requires five heat exchanger functions:

- Condenser.
- Economizer-Subcoolers.
- Liquid-Suction Heat Exchangers.
- Intercooler.
- Evaporator.

For flight hardware, the design goal is to minimize total system weight. The optimum design balances small heat exchanger mass against small internal pressure drops to give the minimum total system mass. Too small heat exchangers will create large internal pressure drops which will require larger power and will in turn require a more massive power supply. The optimum design balances these two competing factors to minimize total system mass.

Our design approach follows. First, we selected the lightest weight, highest performing heat exchanger configuration we know of, which are the flight qualified Hamilton-Standard micro-channel plate-fin heat exchangers. Then, using this basic geometry, for each heat exchanger required in the heat pump system, we designed a series of successively lower pressure drop, but higher weight, options. Next, we analyzed total system performance and the required power supply with the various heat exchanger pressure drops. Finally, we tallied the resulting total system masses to determine the minimum. Briefly, the minimum total system mass occurs with heat exchangers designed to 4 percent pressure drop (i.e., a pressure drop equal to 4 percent of the entering absolute pressure).

6.1 High Performance Micro-Channel Plate Fin Heat Exchangers

Maximum heat exchange for minimum pressure drop occurs by maximizing the surface

area to volume ratio of fluid flow contained in the heat exchanger and by having a large cross-sectional flow area. For flow in a straight line, surface area is wetted perimeter times heat exchanger length; volume is cross-sectional flow area times heat exchanger length. The surface area to volume ratio thus reduces to the ratio of wetted perimeter to cross-sectional flow area. This simple heat exchanger parameter already exists in slightly different form:

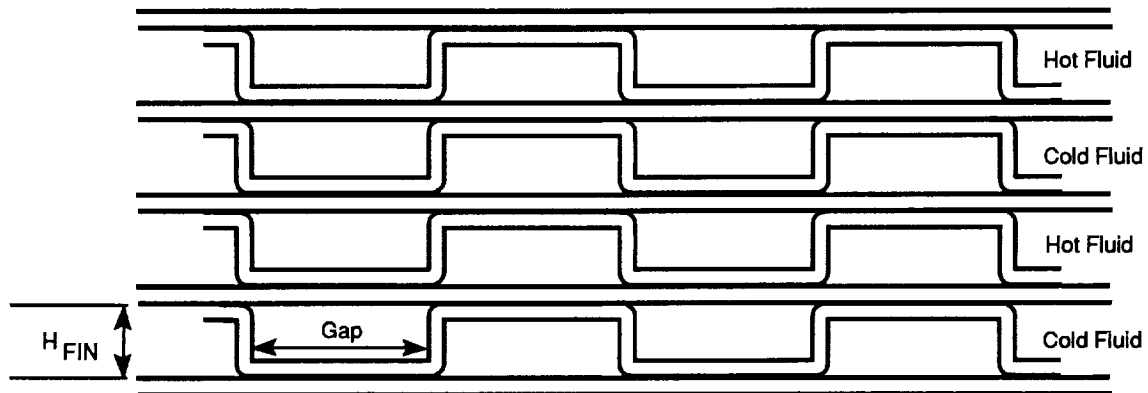
$$\text{Hydraulic Diameter} = \frac{4 \times \text{Cross - Sectional Flow Area}}{\text{Wetted Perimeter}}$$

Clearly, maximizing the surface to volume ratio is equivalent to minimizing the hydraulic diameter of the heat exchanger flow channels. Configuring a heat exchanger with a sufficiently small hydraulic diameter minimizes weight for any desired level of heat exchange. Providing sufficiently large cross-sectional flow area reduces pressure drop, but adds weight.

Figures 24 and 25 show the Hamilton-Standard plate fin micro-channel geometry that uses thin sheets of metal in a structurally rigid construction. This basic geometry gives designers excellent control over both heat exchanger geometry and hydraulic diameter. The configuration offers inherently high-performance for light weight and also the potential to tune performance and weight as required by varying a few geometrical parameters (i.e., gap width and frontal cross-sectional flow area).

6.2 Heat Transfer and Pressure Drop Correlations

From previous work with refrigerants in our laboratories, we chose the following vapor-liquid correlations to use in our design work. Both the pressure drop and heat transfer correlations use the Martinelli parameter:



- Counter Flow
- Plate Thickness = 0.15 mm (0.006 in.)
- Corrugation = 0.15 mm (0.006 in.)
- H_{FIN} = 0.51 mm (0.020 in.)
- GAP = 0.70 mm (0.028 in.)

241-NAS-9614-6

Figure 24. Cross Section of Heat Exchanger Geometry

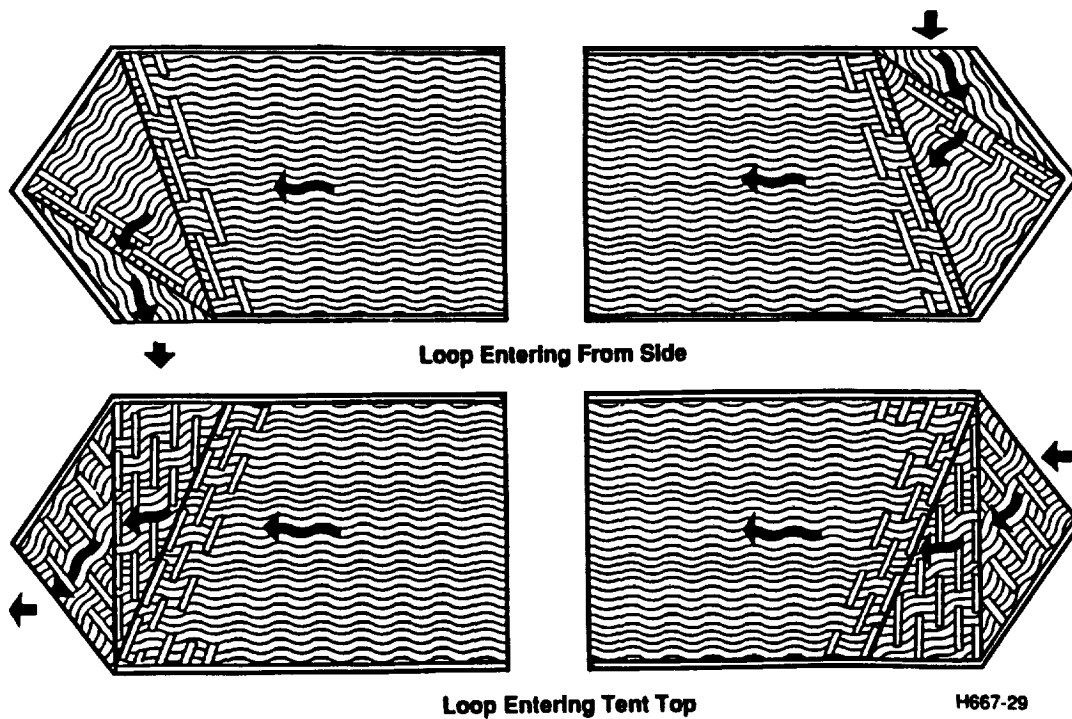


Figure 25. Typical Heat Exchanger Fin Configuration

$$x_{tt} = \left(\frac{\mu_L}{\mu_v} \right)^{0.1} \left(\frac{1-x}{x} \right)^{0.9} \left(\frac{\rho_v}{\rho_L} \right)^{0.5}$$

For frictional pressure drop, we used a correlation by Bae, Maulbetsch, and Rohsenow at M.I.T.

$$\left(\frac{dP}{dZ} \right)_f = \left(\frac{-0.09}{g_o} \right) \frac{G^2}{\rho_v D_H} \text{Re}_v^{-0.2} \left[1 + 2.85 X_{tt}^{0.5235} \right]^2$$

$$D_H = \text{ft}$$

$$G = \text{lbm/ft}^2\text{-hr}$$

$$g_o = 4.17 \times 10^8 \frac{\text{lb}_m - \text{ft}}{\text{lb}_f \text{ hr}^2}$$

For heat transfer, we used a correlation by Traviss, Baron, and Rohsenow, as modified by Foster-Miller's work with refrigerants:

$$F(X_{tt}) = 0.15 \left[X_{tt}^{-1} + 2.85 X_{tt}^{-0.476} \right]$$

$$F_2 = 0.707 \text{Pr}_L \text{Re}_L^{0.5} \quad \text{Re}_L \leq 60$$

$$F_2 = 5 \left\{ \text{Pr}_L + \ln \left[1 + \text{Pr}_L \left(0.09636 \text{Re}_L^{0.585} - 1 \right) \right] \right\} \quad 60 < \text{Re}_L \leq 1125$$

$$F_2 = 5 \text{Pr}_L + 5 \ln(1 + 5 \text{Pr}_L) + 2.5 \ln(0.0031 \text{Re}_L^{0.812}) \quad \text{Re}_L > 1125$$

$$h_{DB} = \frac{K_L}{D_H} 0.023 \text{Re}_L^{0.8} \text{Pr}_L^{0.4}$$

$$h_R = \frac{K_L}{D_H} F(X_{tt}) \text{Pr}_L \text{Re}_L^{0.9} / F_2 \quad 0.1 < F(X_{tt}) \leq 1$$

$$h_R = \frac{K_L}{D_H} [F(X_{tt})]^{1.15} \text{Pr}_L \text{Re}_L^{0.9} / F_2 \quad 1 < F(X_{tt}) < 15$$

$$h_{TP} = 0.025 h_R + 0.00746 h_R^2 + h_{DB} \quad x \leq 0.3$$

$$h_{TP} = 0.192 h_R + 0.00746 h_R^2 \quad x > 0.3$$

6.3 Effect of Heat Exchanger Pressure Drops on COP

The optimum heat exchanger selection will result in minimum total system mass. Making heat exchangers too small (in an effort to save heat exchanger mass) will result in large pressure drops which significantly reduce system COP. The lowered COP will mean increasing power supply mass to the point where it outweighs the heat exchanger mass savings. Conversely, making heat exchangers with negligible pressure drops (in an effort to keep COP at a maximum) will necessitate unwarranted heat exchanger mass. A trade study between heat exchanger efficiency and total system mass helped minimize total system mass.

To analyze the effect of heat exchanger efficiency on total system mass, Foster-Miller first analyzed the effect of heat exchanger pressure drop on system COP. Figure 26 shows the simultaneous effect, for various candidate three stage heat pump cycles, of the pressure drops of ALL heat pump heat exchangers on cooling COP. Next, for each heat exchanger in the heat pump, we designed configurations with 0.5 percent, 1 percent, 2 percent, 4 percent, 6 percent, and 10 percent core pressure drop losses. The higher pressure drop configurations weighed successively more. Figure 27 plots mass versus pressure drop for all these heat exchanger configurations in a three stage CFC-11 heat pump.

With information from Figures 24 through 27, we calculated total system mass for heat pumps of varying heat exchanger efficiency. Namely, selecting one heat exchanger pressure drop determines total core heat exchanger mass and heat pump COP. The COP determines the power system mass. Adding all other masses yields

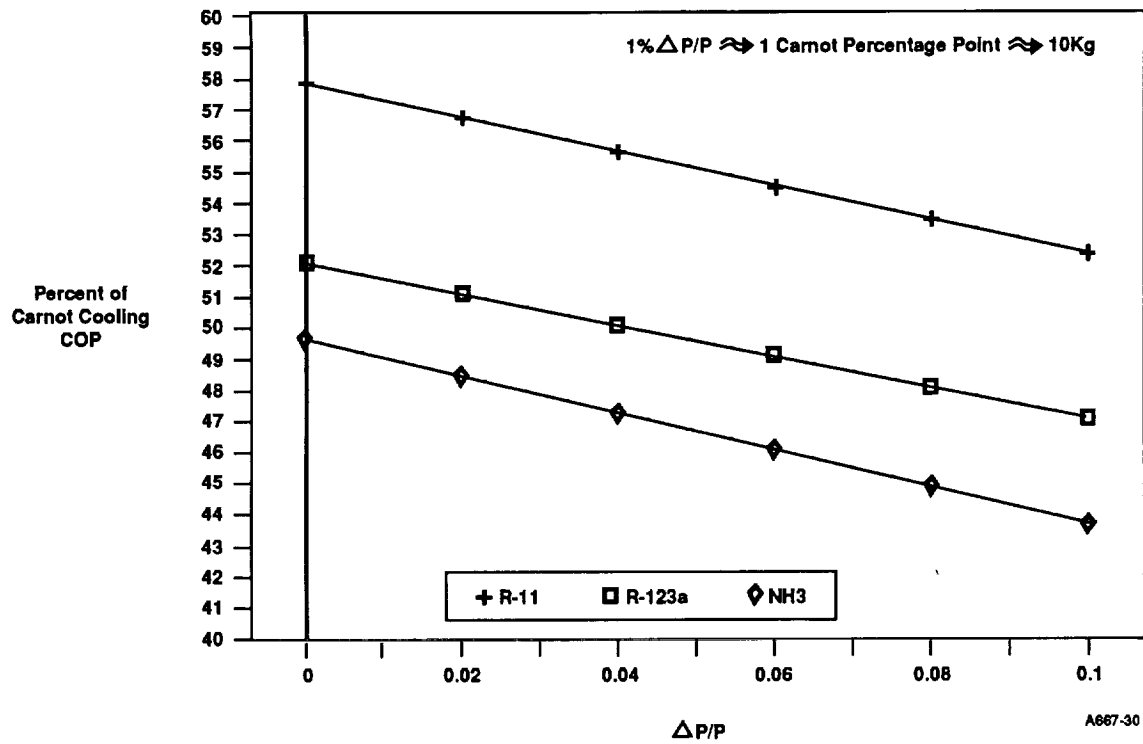


Figure 26. Effect of All Heat Exchanger Pressure Drops on COP for Three-Stage Cycles

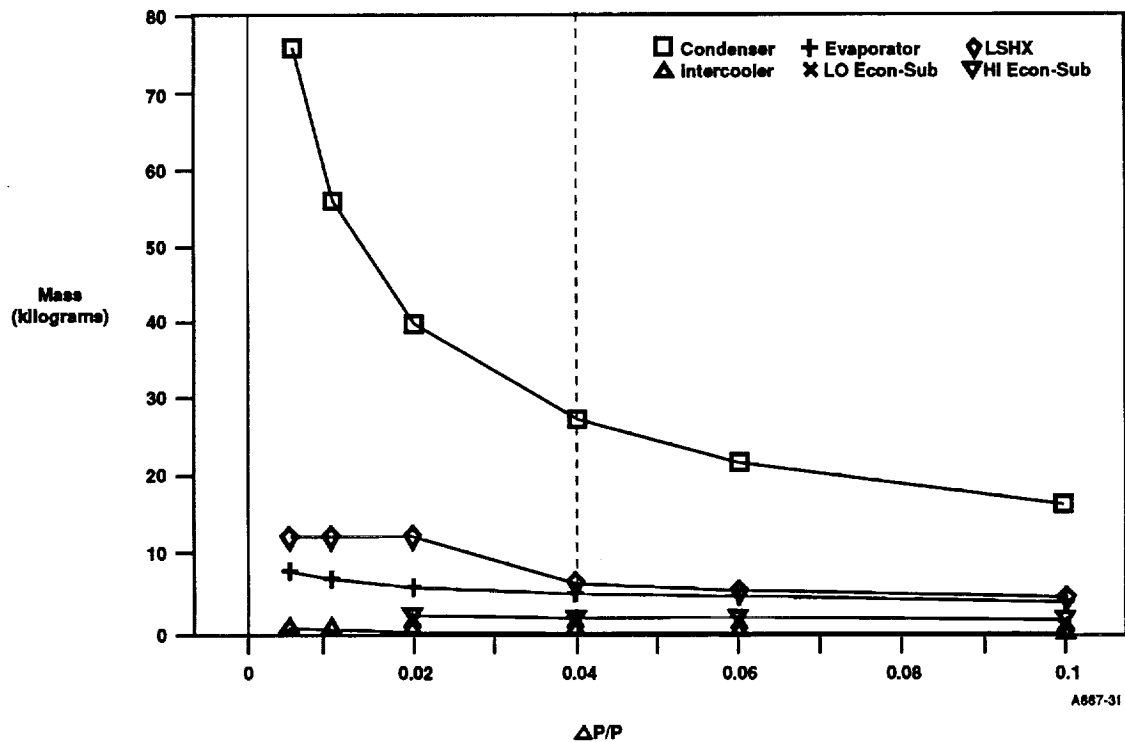


Figure 27. Core Heat Exchanger Mass as a Function of Pressure Drop

total system mass. Table 13 shows total system mass and component masses for the Lunar Base heat pump. Table 14 shows total system mass and component masses for the Lunar Lander. In each case, four percent heat exchanger pressure loss throughout the heat pump minimizes total system mass. Tables 15 and 16 show individual heat exchanger masses respectively for the Lunar Base and Lunar Lander, each at the four percent pressure drop condition.

Tables 13 and 14 showed that system mass reaches a minimum at four percent heat exchanger pressure drop for both the Lunar Base and the Lunar Lander. This means that every

heat exchanger in the heat pump has an outlet pressure four percent less than its inlet pressure. Several things should be noted from the tables. First, heat exchanger pressure drop does not greatly affect system mass. Next, all heat exchangers are held at the same percentage pressure loss. Ultimate design optimization may have different percentage pressure losses at each heat exchanger. Figure 27 shows that both economizer-subcoolers, the evaporator, and the intercooler could operate at two percent pressure loss or less with very little mass increase. Here lighter power system mass realized from the higher COP could offset the slight heat exchanger mass penalty.

Table 13. Lunar Base Parameters for Different Pressure Drops

Percent		Kilograms				
$\Delta P/P$	Carnot COP	Radiator and Power Mass	Heat Exchangers	Compressors	Packaging	Total
2	56.6	858.62	62.5	61	18.53	1001
4	55.5	868.20	43.15	61	15.62	988
6	54.3	879.55	36.54	61	14.63	992

Table 14. Lunar Lander Parameters for Different Pressure Drops

Percent		Kilograms				
$\Delta P/P$	Carnot COP	Radiator and Power Mass	Heat Exchangers	Compressors	Packaging	Total
2	47.2	192.93	15.75	30	6.86	246
4	45.8	196.93	11.05	30	6.16	244
6	44.8	199.84	9.29	30	5.89	245

Table 15. Lunar Base Heat Exchanger Description

Heat Exchanger	H _{FIN} (mm)	N _{CELLS}	Area (m ²)	W (cm)	H (cm)	L (cm)	MASS (kg)
Condenser	0.508	3,000	12.54	6.5	6.5	173	27.65
Econ-Sub HI	0.508	745	0.92	3.2	3.2	51	2.04
Econ-Sub LO	0.508	985	0.76	3.7	3.7	32	1.69
Evaporator	0.508	9,125	2.33	11.3	11.3	11	5.12
LSHX	0.508	12,000	2.86	12.9	12.9	10	6.28
Intercooler	0.508	957	0.17	3.7	3.7	7	0.37

Table 16. Lunar Lander Heat Exchanger Description

Heat Exchanger	H _{FIN} (mm)	N _{CELLS}	Area (m ²)	W (cm)	H (cm)	L (cm)	MASS (kg)
Condenser	0.508	740	3.29	3.2	3.2	184	7.34
Econ-Sub	0.508	855	0.52	3.5	3.5	25	1.17
Evaporator	0.508	1,825	0.47	5.0	5.0	11	1.02
LSHX	0.508	2,600	0.69	6.0	6.0	11	1.52

7. HEAT PUMP CONTROLS

7.1 Control Parameters and Requirements

The purpose of the heat pump controls is to regulate the operation of the heat pump during off-design conditions so that the correct operating point is maintained. The heat pump must maintain the temperature of the cooling water loop at $277\text{K} \pm 2\text{K}$. This temperature condition must be achieved over a heat rejection load variation of 0 to 100 percent. Also affecting the operation of the heat pump is the extreme variation seen in the condensing temperature which can change for a lunar application from 277 to 387K.

Another important aspect which has implications for the heat pump control is the need

for operating redundancy for critical components, such as the heat pump compressors. The criterion used in the design of the heat pump is that the system must be capable of operating at 80 percent of capacity with one compressor failure and at 40 percent of capacity with two failures.

7.2 Description of Control Approach

Figure 28 shows a general schematic of the heat pump with the major system control elements. For the purpose of redundancy, the compressor requirement for each stage has been divided over three units that are sized such that only two compressors at each stage are needed to meet approximately 80 percent of the design capacity. The remaining three compressors are

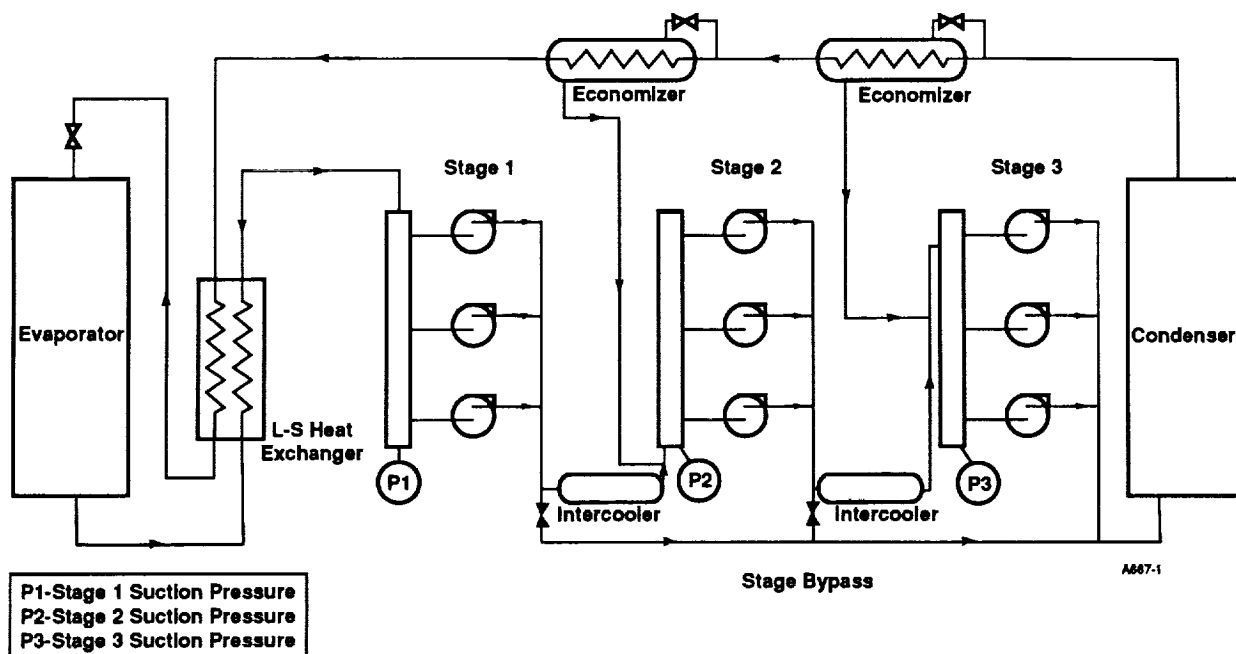


Figure 28. Flow Diagram of the Lunar Heat Pump with Control Points

needed only for full load heat rejection at the highest condensing temperature. For other operating conditions, these three compressors can be considered redundant.

Dividing the compressor capacity over multiple units also provides a means of capacity control with varying thermal rejection load and condensing temperature. The approach is referred to as multiplexing and is commonly used in large commercial refrigeration systems such as those employed in supermarkets. In a multiplexed system, the number of compressors operating at any given time is chosen to match the compressor capacity with the load. Compressors are controlled by on/off compressor cycling, or in the more advanced version suggested here, variable speed operation of several of the compressors can also be employed.

The control of either the compressor cycling or speed is based upon the suction pressure value. Rising suction pressure indicates that the capacity of the compressors operating is less than required. The response to the rise is either an increase in compressor speed or the addition of another compressor if the speed of all running compressors is the maximum. A drop in suction pressure shows that the compressor capacity is greater than that required for the heat load. The compressor speeds are decreased until the minimum allowable speed is reached; at that point, a compressor is cycled off to decrease capacity further.

The multiplex approach can be used for all compressor stages. The interstage pressures become control points for the second and third stage compressors since the interstage pressure between the first and second stages is the suction pressure of the second stage and the interstage pressure between the second and third stage is the suction pressure of the third stage compressors. Changes in these interstage pressures also represent compressor capacity variation and can be used to adjust both compressor speed and cycling.

Application of multiplexing for the high-lift heat pump can be described as follows. The evaporator suction and two interstage pressures will be employed as the control points for the three compressor stages. Pressure set points will

be maintained for each of these pressures within an allowable control bandwidth. The size of this bandwidth will be established during laboratory testing of the heat pump. Compressor control will be done by a combination of on/off cycling and variable speed operation. All compressors will be equipped with variable speed capability to give maximum flexibility and redundancy to their operation. During operation, a change in pressure value will force a response by the compressors. In the case of decreasing pressure, the operating compressors will reduce speed until a minimum speed limit is reached. At that point, one of the operating compressors will be cycled off and the speed of the remaining compressors will be adjusted upward. If further capacity reduction is required, the speed of the remaining compressors will again be lowered until the pressure criteria is met or a second compressor must be cycled off. The minimum operating condition for any stage is, therefore, one compressor operating at the minimum allowable speed. For an increasing pressure situation, the opposite approach is initiated. The speed of all operating compressors is increased until the maximum speed is reached. Further pressure rise requires that a compressor be cycled on and the speed of all compressors be adjusted accordingly. The maximum operating case is all compressors running at maximum speed.

System control must also be applied to compensate for the large variation in condensing temperature seen over the lunar day. The impact of this change is shown in Figure 29. Three stages of compression are needed for heat rejection during the time period of approximately 0 to 40 deg of lunar noon. From 40 to 70 deg, the condensing temperature has dropped to the point where only two stages of compression are needed, while from 70 deg to the beginning of lunar night, one stage of compression is adequate.

At the point of 40 and 70 deg, the control consists of simply cycling off all compressors associated with either the third or second stage, respectively. During intermediate operation, two possible control scenarios exist. The first consist of simply allowing the pressure ratio of the upper operating stage to reduce as the condensing pressure drops. The second approach is illustrated in Figure 30 and consists of maintaining the upper stages at constant pressure

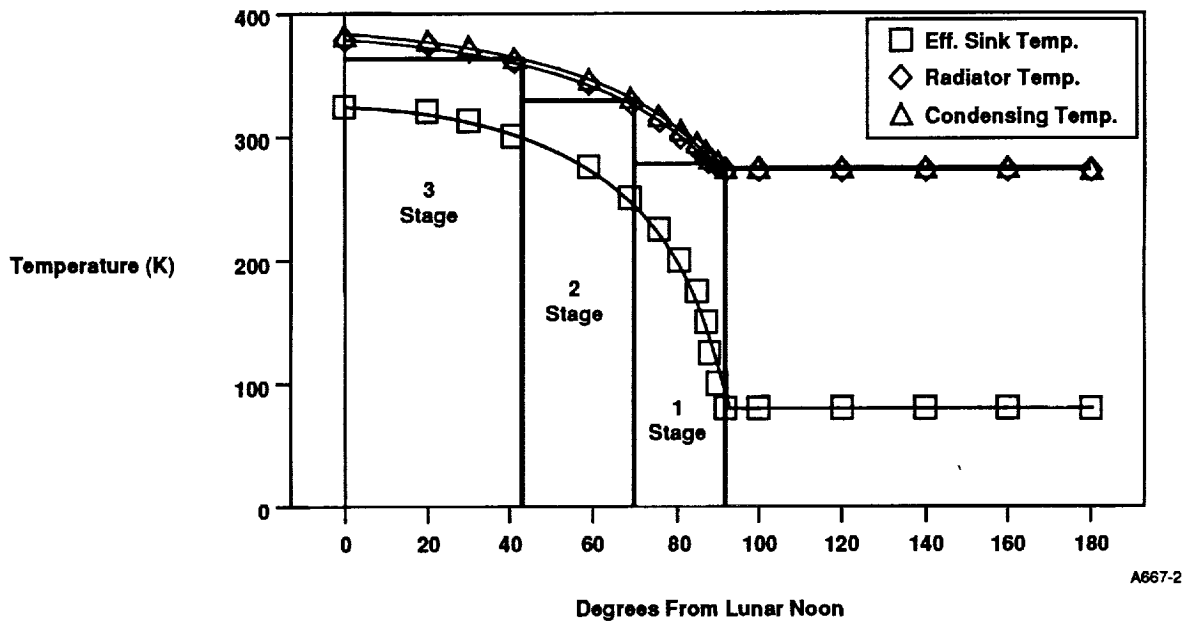


Figure 29. Estimated Heat Pump Condenser Temperature during Lunar Operation

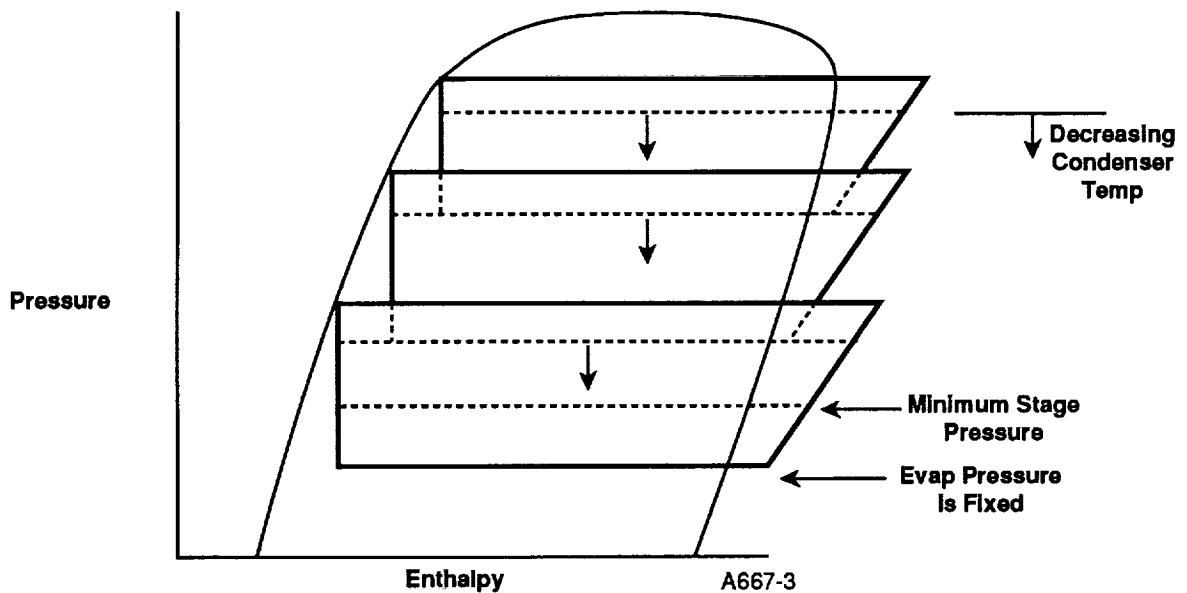


Figure 30. Heat Pump Control Method for Condenser Temperature Change

ratios while reducing the first stage as the condensing temperature decreases. This second approach was found to be more efficient in terms of energy consumption, based on model estimates.

The reduction of the first stage pressure ratio is achieved by varying the interstage pressures as the condensing pressure decreases. This can be achieved using the multiplexing approach described above with new interstage set points. When the condensing pressure decreases, the second and third stage interstage pressure set points will be decreased. The multiplexing control will then adjust compressor speed and cycling as needed to meet these new pressure set points. The first stage pressure ratio will be decreased until a value of 2.0 is reached, which should correspond to the point where the upper most stage is shut down. After shutdown, the interstage pressure is reset to a value appropriate for the remaining stages. The control of interstage pressure continues as described until

single stage operation is reached. At that point the pressure ratio is allowed to decrease with the condensing pressure until a predetermined minimum is reached when heat pump operation is terminated and direct heat rejection is employed.

Heat pump start up is the reverse of this process. Initial operation is in the single stage mode until the condensing temperature reaches the point where two-stage compression is required. The interstage pressure is then controlled to optimize energy consumption by maintaining the smallest possible pressure ratio for the first stage. This same process is repeated when the condensing temperature rise causes the third compression stage to be operated.

The lunar lander and the SIRF units would operate using a similar approach with only two stages cycling. The sequence is essentially the same.

8. RISK ANALYSIS

A brief risk analysis was performed during this Phase, but was not intended to be a full Failure Modes and Effect Analysis. The only significant risk was the refrigerant to be used. Table 17 lists the best performing candidates and for each one looks at stability, chemical and thermal, material incompatibilities, toxicity, flammability and acceptable exposure limits.

CFC-11 showed minimal risk as a refrigerant. It exhibited benign behavior relative to chemical stability, toxicity, flammability, and has a high acceptable exposure limit. Areas of concern are thermal stability and elastomer compatibility, both can be dealt with by design. CFC-11 systems are common on earth so numerous components and detail parts are available of compatible materials. No elastomers need to be in the system.

Thermal instability represents a hazard in that CFCs breakdown to toxic chlorine based gases when exposed to fire. This can be accounted for by ensuring that the heat pump is outside of habitat environments. If it is placed in a vacuum environment, it will be unlikely that any fire could be sustained long enough to cause the

transformation to a dangerous gas. If it did, it would be a small quantity escaping harmlessly into the vacuum environment.

For ground processing, technicians would need to follow industry practices to ensure personnel safety.

The best performing "green" refrigerants HCFC-123a/123 have similar safety advantages and concerns as CFC-11, with the addition of lower acceptable exposure limits. Neither of these is an unworkable concern however. The low acceptable exposure limits are due primarily to conservatism as the refrigerants are new and relatively unknown. They have also been shown to cause benign tumors in laboratory rats at relatively high exposure levels. The small quantity used in this heat pump should not create exposure levels exceeding the recommended limits. It cannot create any significant level for a time approaching the 8 hr associated with the exposure limit.

Again for ground processing, technicians would need to follow industry practices to ensure personnel safety.

Table 17. Refrigerant Safety Tradeoff Matrix

Refrigerant	Stability			Incompatible With	Toxic			Flammable	Acceptable Exposure (ppm)
	Chem	Thermal	Bad		Skin	Eye	Lung		
CFC-11	Ok	Hazard	-	Elastomers	No	Min	No	No	1000
HCFC-123/123a		Hazard	-	Elastomers	No	Min	Yes	Mixture w/air	10
HFC-134a	Ok	Hazard	-	Elastomers	No	Min	No	No	1000
NH ₃	Ok	Ok	Ok	Some metal halogens	Min	Yes	Yes	Mixtures w/air	50
H ₂ O	Ok	Ok	Ok		No	No	No	No	
FC-72	Ok	Hazard	Fair	Plastics, elastomers	Min	No	Min	Vapors	
FC-75	Ok	Hazard	Fair	Plastics elastomers	Min	No	No	Vapors	
n-Butane	Ok	Ok	Ok		Min	Min	No	Yes	1000

9. RECOMMENDATION

A heat pump can be designed and implemented using current technology and meeting the requirements of a lunar base and lander. To continue in that direction, Foster-Miller recommends proceeding with the design, manufacture and test of a ground based prototype for the SIRF. Figures 31 and 32 show the SIRF unit physical layout and operating schematic.

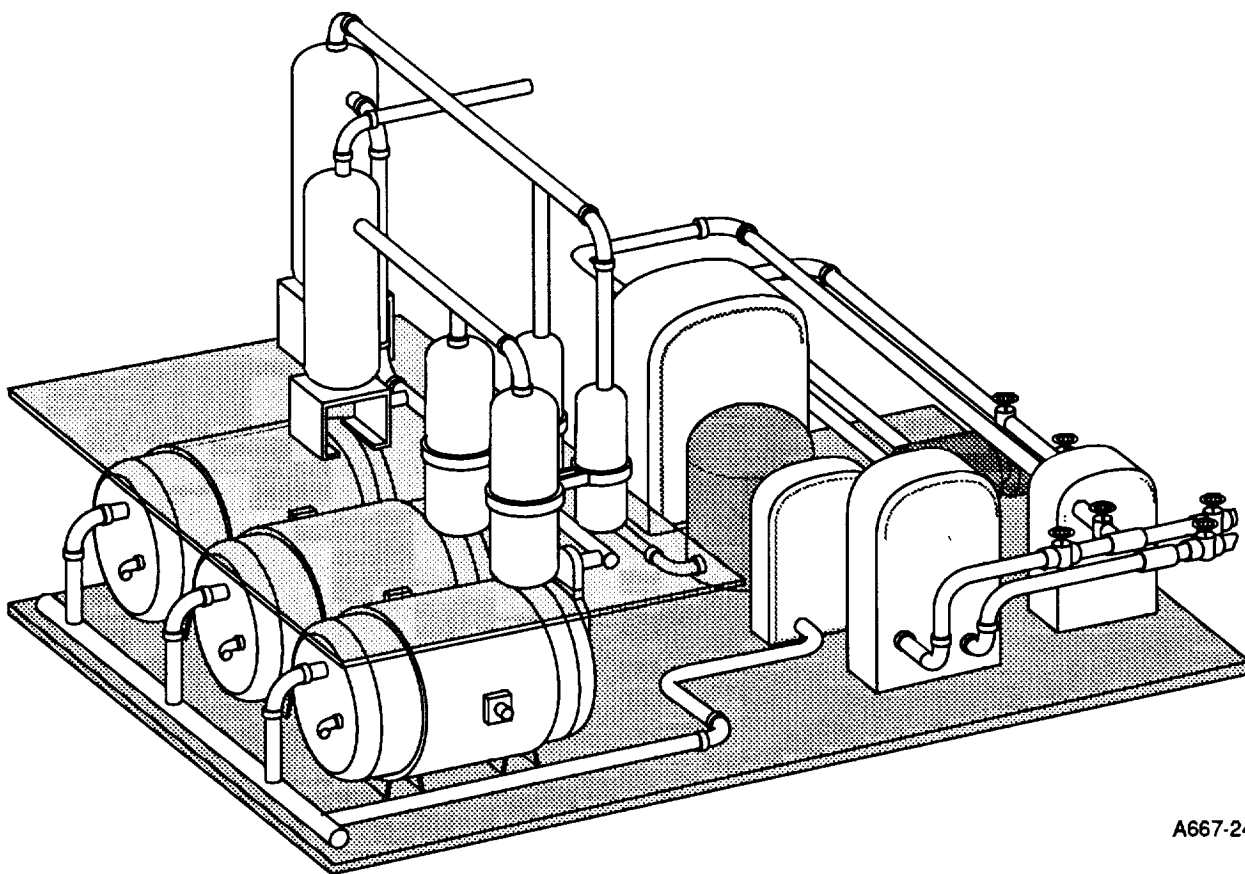
It will consist of a two stage unit using CFC-11 refrigerant. The first stage will consist of three commercial grade scroll compressors, Hitachi Model L500BL. Two will run fixed speed and one variable speed to allow multiplexing for load variation. Oil control will be achieved by commercially available oil separators at the compressor discharges, the compressor oil sumps, an oil reservoir, and oil supply and return lines. The driving forces for oil flow will be provided by existing pressure differential in the heat pump, gravity and internal oil pumping mechanisms in the compressors.

The second stage will consist of two commercial grade rotary (rolling piston) compressors, Mitsubishi Model RL5538EP. One will run fixed speed and one variable speed to allow multiplexing for load variation. Oil control will be similar to stage one, using the

same oil separators, and using the compressor's internal oil pumping and distribution system. The second stage will take advantage of refrigerant liquid injection in the compressor suction line to improve performance and to control compressor temperature for longer life. Liquid refrigerant injection components are commercially available so no component development is required.

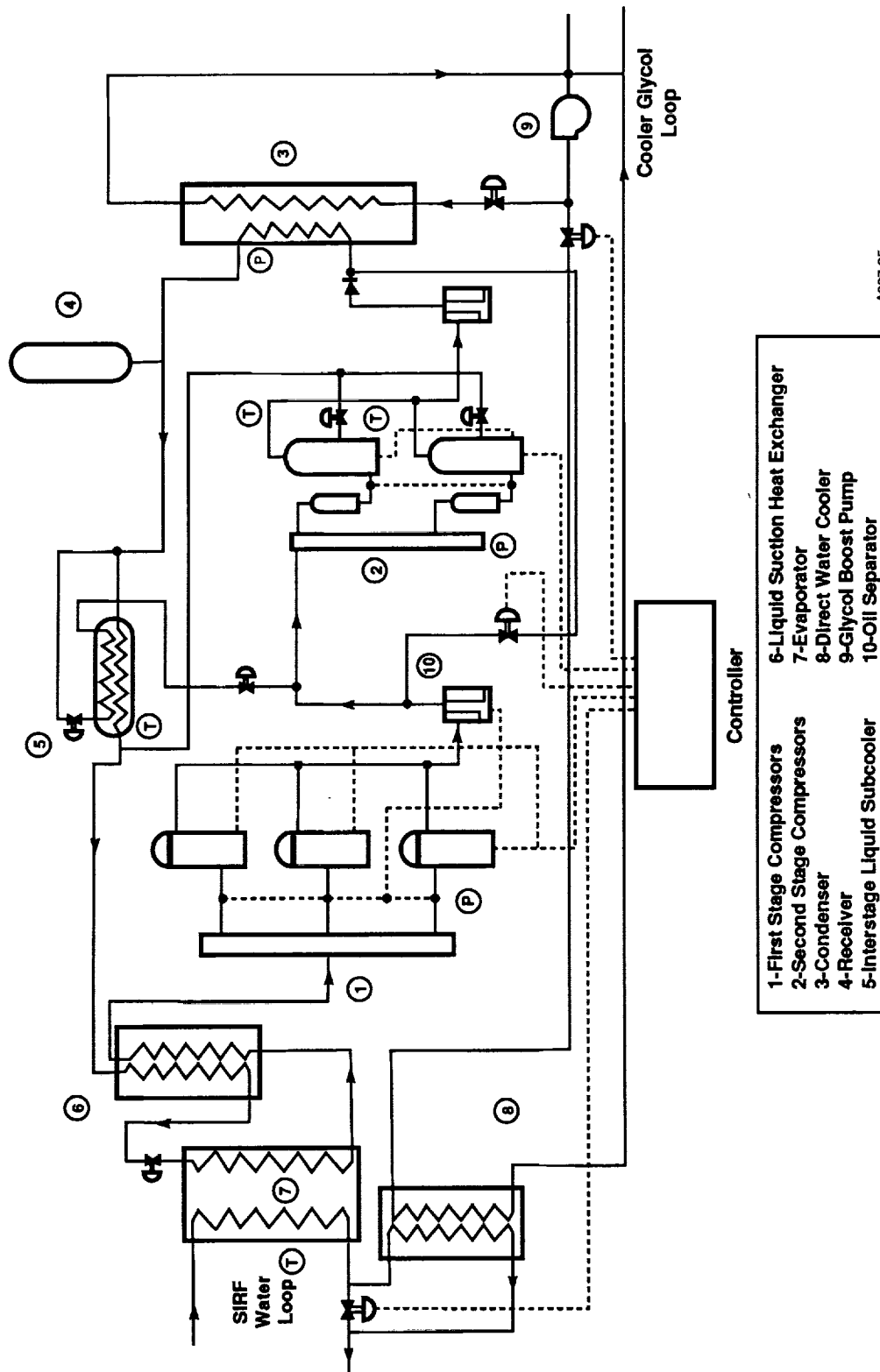
Heat exchangers will all be commercial grade, built to ITT standards. Commercial practices are for manufacturers to build these heat exchangers to order. Therefore lead times are not affected by a manufacturer waiting for a sufficient order to warrant a batch run.

System control will be achieved using a commercial programmable controller to control the appropriate control valves and compressor motors. Control related instrumentation are; the evaporator, interstage and discharge pressures, the water and glycol outlet temperatures, and the liquid and suction refrigerant temperatures. Other instrumentation should include water and flow temperatures for thermal load monitoring, and one Watt transducer per stage to monitor compressor power.



A667-24

Figure 31. SIRF Heat Pump Layout



A667-25

Figure 32. SIRF Heat Pump Diagram

10. REFERENCES

1. *Analysis of Engineering Cycles*, R.W. Haywood, Pergamon Press 1967, LCCCN 66-30628.
2. Mark McLinden, National Institute of Standards and Technology, Boulder, CO.
3. Dave Didion, National Institute of Standards and Technology, Gaithersburg, MD.
4. Jim Sand, Oak Ridge National Laboratory.
5. Balje, O.E., A Study on Design Criteria and Matching of Turbomachines, Parts A&B, *Journal of Engineering for Power*, Jan. 1962
6. Dexter, P.F., et al, "Vapor Cycle Compressors for Aerospace Vehicle Thermal Management," SAE Tech. Paper 901960
7. ASHRAE Handbook: Equipment; Amer. Soc. of Heating, Refrigerating, and Air-Conditioning Engineers, Inc., Atlanta, GA 30329.

APPENDIX A

LUNAR BASE HEAT PUMP AT NIGHT

PRECEDING PAGE BLANK NOT FILMED

APPENDIX A

LUNAR BASE HEAT PUMP – AT NIGHT

(Calculation of necessary radiator area)

GOAL: calculate minimum required radiator area for passive heat rejection.

DESIGN CONDITIONS

Cooling water loop:

Heat to be rejected:

$$Q_{rej} := 5 \cdot \text{kW}$$

Water temperatures:

$$T_{water_in} := 307 \cdot \text{K}$$

$$T_{water_out} := 277 \cdot \text{K}$$

ASSUMED END-OF-LIFE EQUIPMENT PERFORMANCE

Thermal bus:

$$T_{bus} := T_{water_out} - 2 \cdot \text{K}$$

Radiators:

Stefan-Boltzmann constant:

$$\text{emissivity: } \epsilon = 0.9$$

$$\sigma = 5.67 \cdot 10^{-8} \frac{\text{watt}}{\text{m}^2 \cdot \text{K}^4}$$

$$\text{fin efficiency: } \eta = 0.8$$

an effective radiant sink temperature includes the effect of the assumed end-of-life visible light absorptivity, 0.23, and of view factor of the lunar surface:

$$T_{eff} = 80 \cdot \text{K} \quad \text{during the whole lunar night.}$$

operating temperature:

$$T_{rad} := T_{bus} - 2 \cdot \text{K}$$

RESULTING SYSTEM PERFORMANCE

Total heat leaving radiator:

$$Q_{rad} := Q_{rej}$$

$$Q_{rad} = 5 \cdot \text{kW}$$

Required radiator area:

$$A_{rad} := \frac{Q_{rad}}{\epsilon \cdot \eta \cdot \sigma \cdot (T_{rad}^4 - T_{eff}^4)}$$

$$A_{rad} = 22.21 \cdot \text{m}^2$$

RESULTING RADIATOR WEIGHT

Radiator mass per unit *radiating* area:

$$\text{mass_per_rad_area} = 3.85 \frac{\text{kg}}{\text{m}^2}$$

Radiator weight:

$$\text{mass}_{rad} := A_{rad} \cdot (\text{mass_per_rad_area})$$

$$\text{mass}_{rad} = 85.52 \cdot \text{kg}$$

LUNAR BASE HEAT PUMP – AT NOON

(Design point optimization)

GOAL: select radiator design temperature for minimum total system weight.

DESIGN CONDITIONS

Cooling water loop:

Heat to be rejected:

$$Q_{rej} := 5 \cdot \text{kW}$$

Water temperatures:

$$T_{\text{water_in}} := 307 \cdot \text{K}$$

$$T_{\text{water_out}} := 277 \cdot \text{K}$$

ASSUMED END-OF-LIFE EQUIPMENT PERFORMANCE

Thermal bus:

$$T_{\text{bus}} := T_{\text{water_out}} - 2 \cdot \text{K}$$

Radiators:

$$\text{emissivity: } \epsilon = 0.9$$

Stefan-Boltzmann constant:

$$\sigma = 5.67 \cdot 10^{-8} \frac{\text{watt}}{\text{m}^2 \cdot \text{K}^4}$$

$$\text{fin efficiency: } \eta = 0.8$$

An effective radiant sink temperature includes the effect of the assumed end-of-life visible light absorptivity, 0.23, and of view factors of both sun lunar surface:

$$T_{\text{eff}} = 325 \cdot \text{K} \quad \text{at lunar noon, the worst-case condition.}$$

Minimum required radiator area (previous calculation) for passive night operation:

$$A_{\text{night}} = 22.21 \cdot \text{m}^2$$

For this study, vary design radiator temperature to see its effect on system weight:

$$T_{\text{RadMin}} = 335 \cdot \text{K}$$

$$T_{\text{RadMax}} = 450 \cdot \text{K}$$

$$T_{\text{rad}} := T_{\text{RadMin}} + T_{\text{RadMax}}$$

From here on, therefore, express all relevant design conditions as a function of T_{rad} .

$$\text{For example: } T_{\text{bus}} = f(T_{\text{rad}}) = T_{\text{bus}}(T_{\text{rad}})$$

$$\text{Thermal bus: } T_{\text{bus}}(T_{\text{rad}}) := T_{\text{rad}} + 2 \cdot \text{K}$$

$$\text{Heat Pump: } T_{\text{hot}}(T_{\text{rad}}) := T_{\text{bus}}(T_{\text{rad}}) + 2 \cdot \text{K}$$

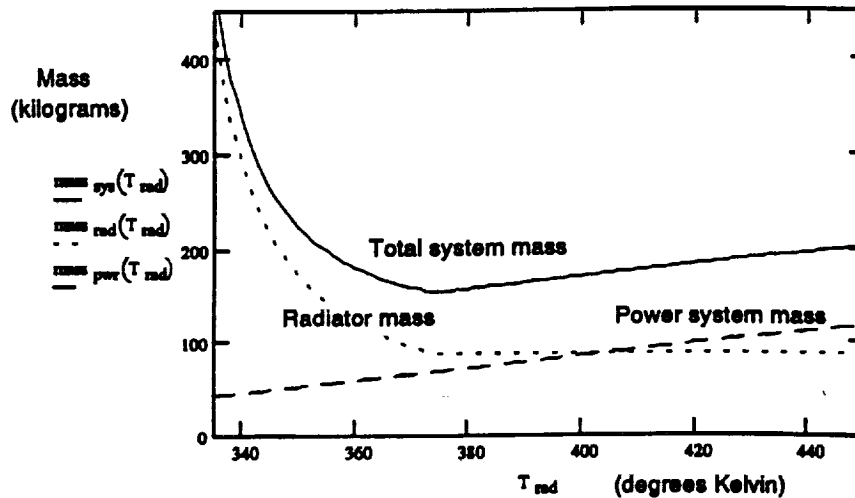
$$T_{\text{cold}} := T_{\text{water_out}} - 2 \cdot \text{K}$$

assume COP as percentage of ideal Carnot:

$$\text{COP}_{\text{cool}}(T_{\text{rad}}) := \frac{T_{\text{cold}}}{T_{\text{hot}}(T_{\text{rad}}) - T_{\text{cold}}} \cdot (\text{pct_Carnot})$$

EFFECT OF RADIATOR DESIGN TEMPERATURE ON SYSTEM WEIGHT

Mass as a function of Radiator Temperature



Designing for minimum system mass requires a noon-time radiator optimum temperature of:

$T_{rad_opt} := 374 \text{ K}$ which gives the following design conditions at T_{rad_opt} :

$$\begin{aligned} T_{hot}(T_{rad_opt}) &= 378 \text{ K} \\ T_{cold} &= 275 \text{ K} \end{aligned}$$

$$\begin{aligned} COP_{cool}(T_{rad_opt}) &= 1.87 \\ KW_{pwr}(T_{rad_opt}) &= 2.68 \text{ kW} \end{aligned}$$

$$A_{rad}(T_{rad_opt}) = 22.36 \text{ m}^2$$

$$\begin{aligned} mass_{pwr}(T_{rad_opt}) &= 66.88 \text{ kg} \\ mass_{rad}(T_{rad_opt}) &= 86.08 \text{ kg} \\ mass_{sys}(T_{rad_opt}) &= 152.97 \text{ kg} \end{aligned}$$

Assumed $pct_Carnot = 70 \%$

Effective radiant sink temperature:

$$T_{eff} = 325 \text{ K}$$

Power mass penalty:

$$mass_per_kW = 25 \frac{\text{kg}}{\text{kW}}$$

Radiator mass per unit area:

$$mass_per_rad_area = 3.85 \frac{\text{kg}}{\text{m}^2}$$

$$\text{Radiator area required at night: } A_{night} = 22.21 \text{ m}^2$$

Clearly, the radiator area required for passive night operation determines the optimum noon-time radiator design temperature for minimum system mass.

REPORT DOCUMENTATION PAGE

Form Approved
OMB No. 0704-0188

Public reporting burden for this collection of information is estimated to average 1 hour per response, including the time for reviewing instructions, searching existing data sources, gathering and maintaining the data needed, and completing and reviewing the collection of information. Send comments regarding this burden estimate or any other aspect of this collection of information, including suggestions for reducing this burden, to Washington Headquarters Services, Directorate for Information Operations and Reports, 1215 Jefferson Davis Highway, Suite 1204, Arlington, VA 22202-4302, and to the Office of Management and Budget, Paperwork Reduction Project (0704-0188), Washington, DC 20503.

1. AGENCY USE ONLY (Leave blank)		2. REPORT DATE July 1994		3. REPORT TYPE AND DATES COVERED Phase I Final Report 1/20/93 - 5/18/93	
4. TITLE AND SUBTITLE Lunar Base Heat Pump				5. FUNDING NUMBERS 92143001A(N)	
6. AUTHOR(S) J. Goldman, A. Harvey, T. Lovell, D. Walker					
7. PERFORMING ORGANIZATION NAME(S) AND ADDRESS(ES) Foster-Miller, Inc. 350 Second Avenue Waltham, MA 02154-1196				8. PERFORMING ORGANIZATION REPORT NUMBER NAS-8819-FM-9614-820	
9. SPONSORING/MONITORING AGENCY NAME(S) AND ADDRESS(ES) NASA Lyndon B. Johnson Space Center Houston, TX 77058				10. SPONSORING/MONITORING AGENCY REPORT NUMBER NAS9-18819	
11. SUPPLEMENTARY NOTES NASA Lyndon B. Johnson Space Center; Attention: John D. Cornwell, EC2 Houston, TX 77058					
12a. DISTRIBUTION/AVAILABILITY STATEMENT Rights to this data shall be in accordance with Clause 52.227-20				12b. DISTRIBUTION CODE N/A	
13. ABSTRACT (Maximum 200 words) This report describes the Phase I process and analysis used to select a refrigerant and thermodynamic cycle as the basis of a vapor compression heat pump requiring a high temperature lift, then to perform a preliminary design to implement the selected concept, including major component selection. Use of a vapor compression heat pump versus other types was based on prior work performed for the Electric Power Research Institute. A high lift heat pump is needed to enable a thermal control system to remove heat down to 275K from a habitable volume when the external thermal environment is severe. For example, a long-term lunar base habitat will reject heat from a space radiator to a 325K environment. The first step in the selection process was to perform an optimization trade study, quantifying the effect of radiator operating temperature and heat pump efficiency on total system mass; then, select the radiator operating temperature corresponding to the lowest system mass. Total system mass included radiators, all heat pump components and the power supply system. The study showed that lunar night operation, with no temperature lift, dictated the radiator size. To operate otherwise would require a high mass penalty to store power. With the defined radiation surface, and heat pump performances assumed to be from 40 percent to 60 percent of the Carnot ideal, the optimum heat rejection temperature ranged from 387K to 377K, as a function of heat pump performance. Refrigerant and thermodynamic cycles were then selected to best meet the previously determined design conditions. The system was then adapted as a ground-based prototype lifting temperature to 360K (versus 385K for flight unit) and using readily available commercial-grade components. Over 40 refrigerants, separated into wet and dry compression behavioral types, were considered in the selection process. Refrigerants were initially screened for acceptable critical temperature. The acceptable refrigerants were analyzed in ideal single and two-stage thermodynamic cycles. Top candidates were analyzed assuming realistic component limits and system pressure drops, and were evaluated for other considerations such as safety, environmental impact and commercial availability. A maximum coefficient of performance (COP) of 56 percent of the Carnot ideal was achievable for a three-stage CFC-11 cycle operating under the flight conditions above. The program was completed by defining a control scheme and by researching and selecting the major components, compressor and heat exchangers, that could be used to implement the thermodynamic cycle selected. Special attention was paid to using similar technologies for the SIRF and flight heat pumps resulting in the commercially available equivalent of the flight unit. A package concept was generated for the components selected and mass and volume estimated.					
14. SUBJECT TERM High temperature lift, Heat pumps, Refrigerant selections, Compressors				15. NUMBER OF PAGES 68	
				16. PRICE CODE N/A	
17. SECURITY CLASSIFICATION OF REPORT Unclassified	18. SECURITY CLASSIFICATION OF THIS PAGE Unclassified	19. SECURITY CLASSIFICATION OF ABSTRACT Unclassified	20. LIMITATION OF ABSTRACT Unlimited ✓		

NSN 7540-01-280-5500

Standard Form 298 (Rev. 2-89)
Prescribed by ANSI Std. Z39-18

